DAYLIGHT MODELLING AND OPTIMIZATION OF SOLAR FACADES

Eero Vartiainen

Dissertation for the degree of Doctor of Science in Technology to be presented with due permission of the Department of Engineering Physics and Mathematics, for public examination and debate in Auditorium F1 at Helsinki University of Technology (Espoo, Finland) on the 26th of January, 2001, at 12 o'clock noon.

Helsinki University of Technology

Department of Engineering Physics and Mathematics

Laboratory of Advanced Energy Systems

Teknillinen korkeakoulu

Teknillisen fysiikan ja matematiikan osasto

Teknillinen fysiikka – energiateknologiat

PREFACE

Helsinki, December 12th, 2000

Eero Vartiainen

ABSTRACT

Improved daylighting is an efficient way of utilizing solar energy in buildings. It is relatively cheap and more efficient than common electric incandescent or fluorescent light. Daylight can be utilized with traditional facades with wall windows, skylight windows, or with multifunctional photovoltaic (PV) solar facades which can produce daylight, heat, and electricity for the building. In this thesis, the optimal use of daylight in solar facades is studied. A new daylight simulation tool, DeLight, developed in the Helsinki University of Technology, is used for the daylight calculations and optimizations. It is a more accurate tool than the simple daylight factor models but faster than the more sophisticated models commercially available.

The simulation tool DeLight uses a single room two-zone model with one wall window. It takes as input data hourly horizontal beam and diffuse irradiance measurements which are readily available at many weather stations around the world. The irradiance measurements are converted to illuminance values by the Perez luminous efficacy model, and the illuminance values are used to generate a sky luminance distribution by the Perez all-weather sky luminance model, because these models were found to agree best with year-round illuminance and irradiance measurements. The interior illuminance distribution is calculated from the room geometry and the sky luminance distribution by an interior light transfer model. By simplifying the geometry and omitting higher-order interior reflections, a fast but still accurate simulation tool is achieved. The average simulation error of DeLight is only 2-3% at illuminance levels of 300-500 lx when compared with year-round illuminance and irradiance measurements.

The simulation tool DeLight has been used to assess the daylight availability in a case study room for four facade orientations at four locations. Maximum yearly average daylight availability (*DA*) is achieved with continuous dimming and automated blind system control. About 70-90% of the yearly lighting requirement during the office hours can be provided by daylight in Southern Europe, and 50-70% in Northern Europe. With on/off switching and manual blind control, most of the electricity savings due to daylight are lost. The *DA* can be increased considerably by using diffusive glazing elements near the top of the facade where an outside view is not necessary. However, it is important to also have a clear glazing window at the centre of the facade to permit the occupants visual contact with the environment.

In multifunctional solar facades, the optimization of the window area becomes the key design issue. Increasing the window area reduces the electric lighting load but it also decreases the PV electricity production and increases the heating and cooling load. Considering the yearly total auxiliary energy requirement for heating, cooling, electric lighting, and appliances, the optimum window area is around 15-20% of the total south-oriented facade area. An optimal PV facade layout consists of a central window, diffusive glazing above the window, and PV panels covering the rest of the facade area.

TABLE OF CONTENTS

LIST OF PUBLICATIONS

I   E. Vartiainen, *Daylight modelling with the simulation tool DeLight*, Helsinki University of Technology, Department of Engineering Physics and Mathematics, Report TKK-F-A799, 2000.

II   E. Vartiainen, *An anisotropic shadow ring correction method for the horizontal diffuse irradiance measurements*. Renewable Energy **17** (1999) 311-317.

III   E. Vartiainen, *A comparison of luminous efficacy models with illuminance and irradiance measurements*. Renewable Energy **20** (2000) 265-277.

IV   E. Vartiainen, *A new approach to estimating the diffuse irradiance on inclined surfaces*. Renewable Energy **20** (2000) 45-64.

V   E. Vartiainen, K. Peippo, and P.D. Lund, *Daylight optimization of multifunctional solar facades*. Solar Energy **68** (2000) 223-235.

VI   E. Vartiainen, *Electricity benefits of daylighting and photovoltaics for various solar facade layouts in office buildings*. Energy and Buildings **33** (2000) 113-120.

VII   E.Vartiainen and P.D. Lund, *Daylighting strategies for advanced solar facades*. Proceedings of the 2nd ISES-Europe Solar Congress, EuroSun '98, Portoroz, Slovenia, September 14-17, 1998 (1999) II.3.18.1-6.

VIII E. Vartiainen, *Energy savings from the use of daylight in Finnish non-residential buildings*. Proceedings of the 4th Symposium on Building Physics in the Nordic Countries, Espoo, Finland, September 9-10th (1996) 133-139.

IX   E. Vartiainen, K. Mäki-Petäys, and P.D. Lund, *Daylight measurements and calculations with an a-Si photovoltaic solar facade*. Proceedings of the 3rd ISES-Europe Solar Congress, EuroSun 2000, Copenhagen, Denmark, June 19-22, 2000.

Brief description of the contents of the publications

Publication I documents the theory behind, operation of, and verification of the new daylight simulation model DeLight which has been used for the daylight calculations in this thesis. It also analyses the irradiance measurements which are the basis of the calculations.

Publication II presents a new anisotropic shadow ring correction method for the horizontal diffuse irradiance measurements which are the key input data for the daylight calculations.

Publication III presents a new comparison of various luminous efficacy models with illuminance and irradiance measurements. The best model of this comparison is used for converting the input hourly horizontal irradiance measurements to illuminance values by the simulation tool DeLight.

Publication IV presents a new method to estimate the diffuse irradiance on inclined surfaces and compares different sky luminance and radiance models with comprehensive measurements at 24 surface orientations. The best model of these comparisons is used for generating the sky luminance distribution from the hourly horizontal illuminance values by the simulation tool DeLight.

Publication V analyses the optimal shape, position, and area of a window in a multifunctional solar facade. The optimal division between the window section and the photovoltaic section of the facade is also assessed at four European locations.

Publication VI analyses the electricity benefits of daylighting and photovoltaics in various facade layouts for office buildings at four European locations. The daylight availability and optimal transparent glazing area for the facade layouts is also assessed.

Publication VII analyses the different lighting control strategies for solar facades. The effects of shading systems and electric light control methods on the daylight availability are assessed.

Publication VIII presents a verification study of the simulation tool DeLight and analyses the daylight availability for non-residential buildings at three Finnish locations.

Publication IX presents daylight measurements with a multifunctional solar photovoltaic facade with a window and gaps of clear glazing between the a-Si PV panels.

Author's contribution

I have designed, programmed, and documented the simulation tool DeLight used for the daylight calculations in this thesis. I have written alone all publications and performed all the simulations reported in the publications. I have made the illuminance measurements for publications **I**, **III**, **V**, and **VIII**, made the irradiance measurements for publication **III**, and analysed the results presented in all publications.

NOMENCLATURE

A area of the receiving surface (m^2)

C correction factor for the horizontal diffuse irradiance measurements

C_a anisotropic correction factor for the horizontal diffuse irradiance measurements

C_i isotropic correction factor for the horizontal diffuse irradiance measurements

C_t total correction factor for the horizontal diffuse irradiance measurements

COP coefficient of performance of the cooling system

CU coefficient of utilization

DA yearly average daylight availability during the office hours of the year (%)

DF daylight factor

E horizontal global illuminance (lx)

E_b horizontal beam illuminance (lx)

E_d horizontal diffuse illuminance (lx)

E_{di} diffuse illuminance on an inclined surface (lx)

E_r interior horizontal total illuminance at point R (lx)

$E_{r,b}$ interior horizontal beam illuminance at point R (lx)

$E_{r,d}$ interior horizontal diffuse illuminance at point R (lx)

$E_{r,r}$ interior horizontal reflected illuminance at point R (lx)

$E_{req,b}$ illuminance requirement in the back half of the room (lx)

$E_{req,f}$ illuminance requirement in the front half of the room (lx)

E_v exterior vertical illuminance (lx)

G global horizontal irradiance (W/m^2)

G_d horizontal diffuse irradiance (W/m^2)

G_{di} diffuse irradiance on an inclined surface (W/m^2)

G_{du} uncorrected horizontal diffuse irradiance (W/m^2)

G_λ spectral irradiance (W/m^2nm)

K horizontal global luminous efficacy (lm/W)

K_b horizontal beam luminous efficacy (lm/W)

K_d horizontal diffuse luminous efficacy (lm/W)

K_m luminous efficacy constant for photopic (daytime) vision = 683 lm/W

H horizontal global irradiation (kWh/m^2)

H_b horizontal beam irradiation (kWh/m^2)

H_d horizontal diffuse irradiation (kWh/m^2)

h_r vertical distance between the lower edge of the window and point R (m)

h_w height of the window (m)

I luminous intensity (cd)

L luminance (cd/m^2)

L_p luminance of the point P of the sky (cd/m^2)

l latitude (radians)

MBD   relative mean bias difference (%)

MBRD mean bias relative difference (%)

RMSD relative root mean square difference (%)

RMSRD root mean square relative difference (%)

R_p radiance at point P of the sky (W/m^{2}sr)

U hour angle of the sun (radians from solar noon)

U_0 hour angle at sunset (radians from solar noon)

V view angle of the shadow ring (radians)

V_λ spectral sensitivity of the eye

w_w width of the window (m)

x_r horizontal distance between the left wall and point R (m)

x_w horizontal distance between the left wall and the left edge of the window (m)

z horizontal distance between the window and point R (m)

Greek letters

β inclination angle of the surface (radians)

δ_s declination of the sun (radians)

η_{PV} system efficiency of the PV system (%)

θ_I angle of incidence on the surface (radians)

θ_p altitude angle of point P of the sky (radians)

θ_s solar elevation (radians)

θ_0 minimum of the altitude angle of an inclined surface (radians)

λ wavelength (nm)

τ_w light transmittance of the window

Φ luminous flux (lm)

φ azimuth angle of the point P relative to the normal of the surface (radians)

φ_p azimuth angle of point P of the sky (radians)

φ_s solar azimuth angle (radians)

φ_w azimuth angle of the window normal (radians)

ω solid angle of the receiving surface (sr)

1 INTRODUCTION

1.1 Background

A solar facade is a building component that can utilize the incoming solar radiation. The solar facade can be a conventional wall with windows, allowing daylight and heat into the building. Or, it can be a multifunctional facade producing daylight, heat, and also electricity by photovoltaic (PV) elements in the facade (Fig. 1). In addition to traditional windows, diffusive glazing, transparent insulation, and other advanced daylighting devices can also be used to reduce the need for artificial lighting.
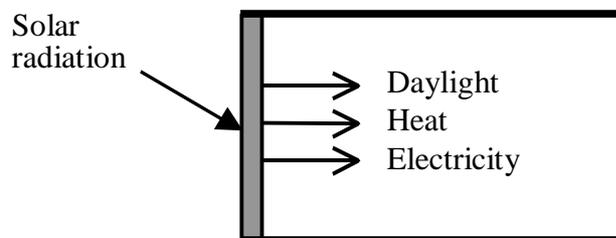
Fig. 1. A multifunctional solar facade producing daylight, heat, and electricity.

Daylighting is an efficient and relatively cheap way of utilizing solar energy in buildings. It has a higher luminous efficacy (lm/W) than common artificial electric incandescent or fluorescent light sources (IESNA, 1993; IEA, 1994). The potential for electricity savings by daylight is considerable; about 25% of the Finnish household electricity consumption goes to artificial lighting (Suomen Sähkölaitosyhdistys, 1995), excluding electric heating. In commercial buildings, electric lighting typically accounts for 30-50% of the electricity consumption (Secker & Littlefair, 1987; Choi & Mistrick, 1997). In office buildings, the lighting requirement usually coincides with daylight hours. It has been estimated that good daylight design, in association with suitable lighting controls, could save over 20% of the energy now consumed by electric lighting in commercial buildings (Lynes, 1996).

Despite the great potential of daylighting, it has received less attention than other solar technologies in the past. The reason for this is that the actual energy savings of daylighting are very difficult to assess. A common way of making daylight calculations is to use a lumen method which is simple enough to permit manual computations. In a

15

lumen method for sidelighting, the interior horizontal daylight illuminance E_r is calculated from the exterior vertical illuminance E_v and the window transmittance τ_w with the help of a coefficient of utilization CU which is determined from a table of coefficients for different room geometries and sky conditions (IESNA, 1993):

$$E_r = E_v \, \tau_w \, CU \,. \tag{1}$$

The major drawback of the lumen method is that it assumes a simplified room geometry where the window extends along the entire window wall from the work plane to the ceiling cavity (Saraiji & Mistrick, 1993). The tabulated CU values are based on measured average illuminances. Moreover, beam sunlight is not allowed to enter the room space.

Another simple daylight calculation method is to use a daylight factor DF as the ratio of the internal daylight illuminance E_r to the external horizontal diffuse illuminance E_d under an overcast sky defined by the CIE luminance distribution (Rutten, 1990):

$$E_r = DF \, E_d \,. \tag{2}$$

The daylight factor method could be correct if the DF were a constant that could be determined beforehand in any circumstances. However, Tregenza (1980) and others have shown that the actual DF is not a constant but can vary by a factor of five. Moreover, the DF does not include the beam sunlight, nor does the lumen method.

For detailed daylight calculations, there exist also computer simulation tools which can handle more complex room geometries and sky conditions than the simple daylight factor and lumen methods. For example, Daylite 2.2, by Solarsoft (USA), can simulate one or all hours of one design day per month (21st) for a standard CIE sky (IEA, 1994). Daylit (USA) uses average monthly weather data and CUs with a mean, overcast, or clear sky (IEA, 1994). DOE-2.1.D (USA) uses the daylight factor method with an interpolation between overcast and clear skies (IEA, 1994). A comprehensive list of the various daylight simulation tools has been done by the International Energy Agency (IEA, 1999).

Two of the most sophisticated simulation models are Superlite and Radiance which have been integrated in the IEA Adeline simulation tool package (University of

California, 1993). With these simulation tools, it is possible to model very complex room geometries and also visualize the interior illuminance distribution. However, these models take a lot of computing time: Superlite takes about 1/2 minute to run one hourly simulation of a complex room on a mainframe computer (IEA, 1994). For Radiance, one hourly simulation with a realistic sky model and minimal interior reflections took more than 2 minutes with a 233 MHz pentium PC (Arpiainen, 1999). The simulation of all hours of one year would take several days with these complex models; it would be almost impossible to solve complicated design problems requiring numerous computer runs. On the other hand, the simpler and less time-consuming models do not generally give sufficiently accurate results. Therefore, it would be useful to have a fast but sufficiently accurate simulation tool for interior daylight calculations.

1.2 The aim of the thesis

The main aim of this thesis has been to optimize daylight utilization in solar facades. For the interior daylight availability analysis and calculations, a new daylight simulation tool, DeLight, was developed which is more accurate than the simple daylight factor models and faster than the more sophisticated models commercially available. The speed of computation is critical because the simulation tool is used to determine the optimal layout and glazing area of multifunctional solar facades at several locations. The overall energy analysis requires numerous year-round simulation runs. Moreover, the simulation tool is used to analyse how the various parameters affecting the daylight availability, e.g., facade orientation, window position, shading system, and electric light control system. From the parametric studies, optimized facade concepts and design guidelines can be determined.

1.3 Modelling approach

A schematic diagram of the daylight simulation model DeLight developed in this study is presented in Fig. 2. A single room model with two lighting zones and one wall window is used. A two-zone model was chosen instead of a single zone room because the daylight illuminance can vary greatly with the distance from the window, and moreover, the lighting requirement can be different in different parts of the room. The model uses hourly horizontal global and diffuse irradiance measurements as input data. These are readily available for many weather stations around the world. The irradiance measurements are converted to illuminance values by a luminous efficacy model. The horizontal illuminance values are in turn used to generate a sky luminance distribution

by a sky luminance model. Finally, the interior illuminance distribution is calculated from the sky luminance distribution and from the room geometry and the position of the sun by an interior light transfer model.

```
┌─────────────────────────────┐
│  Horizontal global and diffuse │
│    irradiance measurements    │
└─────────────────────────────┘
              │
              ▼
        ╭───────────╮
        │  Luminous  │
        │ efficacy model │
        ╰───────────╯
              │
              ▼
┌─────────────────────────────┐
│  Hourly horizontal beam and  │
│  diffuse illuminance values  │
└─────────────────────────────┘
              │
              ▼
        ╭───────────╮
        │    Sky     │
        │ luminance  │
        │   model    │
        ╰───────────╯
              │
              ▼
┌─────────────────────────────┐
│  Sky luminance distribution  │
└─────────────────────────────┘
              │
              ▼
        ╭───────────╮
        │ Interior light │
        │ transfer model │
        ╰───────────╯
              │
              ▼
┌─────────────────────────────┐
│ Interior illuminance distribution │
└─────────────────────────────┘
```
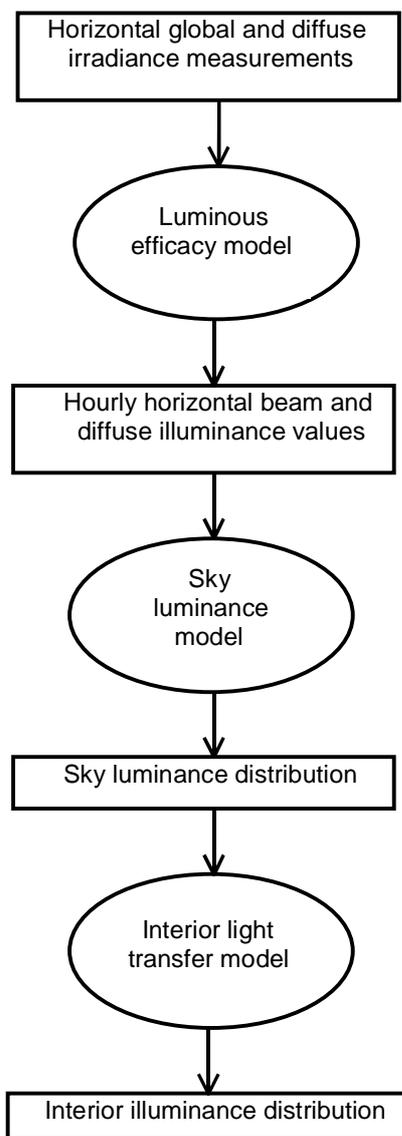
Fig. 2. A schematic diagram of the DeLight daylight simulation model.

The simulation model DeLight is verified (publication **I**) and various luminous efficacy and sky luminance models are tested with year-round illuminance and irradiance measurements. The simulation tool is used to calculate the interior daylight availability for case buildings at different locations. For example, the optimal area of the windows,

electric light control and shading systems can be analysed. Moreover, multifunctional solar facades including windows and PV are optimized to minimize the auxiliary electricity consumption.

The theory of daylight modelling is presented in section 2, including the input irradiance measurements (publication **I**), shadow ring correction of the diffuse irradiance measurements (publication **II**), luminous efficacy models (publication **III**), and sky luminance models (publication **IV**). The simulation tool DeLight is described in section 3 with the verification measurements (publications **I**, **V**). Some applications of DeLight are presented in sections 4 and 5 (publications **V-IX**) and the conclusions in section 6.

2 THEORY OF DAYLIGHT MODELLING

2.1 Solar irradiance measurements

The basis for many interior daylight modelling tools is the hourly horizontal beam and diffuse illuminance (lx) values (IEA, 1994). Unfortunately, these daylight components are measured regularly only at very few locations. However, it is possible to calculate the daylight illuminance values from the horizontal beam and diffuse irradiance measurements (W/m^2) which are readily available for many weather stations around the world. The diffuse daylight component is especially important since it is usually preferred to the beam component for interior illumination purposes. Most of the beam sunlight is usually reflected back, e.g., by Venetian blinds, since it causes discomfort glare for the occupants. However, it could be possible to redirect the beam sunlight by light shelves or other advanced daylighting techniques (Littlefair, 1990).

To get an overview of the solar potential, the yearly horizontal beam, diffuse and global irradiation for some European locations is presented in Table 1 (publication **I**). As can be seen from the table, Sodankylä receives only 27% less diffuse irradiation than Sicily, even though the amount of global irradiation is more than double in Sicily. It seems that the potential for diffuse daylighting is relatively good even north of the Arctic Circle. The amount of beam sunlight is not so important for daylighting, as most of it is usually less wanted or in excess of the lighting requirement (publications **I** and **V**). A thorough analysis of the irradiance measurements used as the input of the daylight model DeLight is presented in publication **I**.

Table 1. The yearly horizontal beam (H_b), diffuse (H_d), and global (H) irradiation (in kWh/m^2) for some European locations. The average of the years 1971-93 has been used for the Finnish locations and the European Test Reference Years for the other locations

Location	Latitude	H_b	H_d	H	$H_d/H_{d,Sicily}$	H/H_{Sicily}
Trapani, Sicily, Italy	37°55'N	1184	632	1816	100%	100%
Paris, France	48°77'N	493	588	1081	93%	60%
London, England	51°47'N	392	540	932	85%	51%
Copenhagen, Denmark	55°46'N	523	492	1015	78%	56%
Helsinki, Finland	60°19'N	429	509	938	81%	52%
Jyväskylä, Finland	62°24'N	405	474	879	75%	48%
Sodankylä, Finland	67°22'N	328	464	792	73%	44%

2.2 Shadow ring correction of the horizontal diffuse irradiance

The horizontal diffuse irradiance is usually measured with a shadow ring which prevents the beam radiation from entering the measuring equipment. However, the shadow ring also blocks part of the diffuse sky radiation. Therefore, to account for the shaded part of the sky, the measured diffuse irradiance G_{du} has to be adjusted by a correction factor C:

$$G_d = C\, G_{du} \tag{3}$$

where G_d is the corrected value of the horizontal diffuse irradiance. The correction is usually made by assuming that the sky radiance distribution is isotropic. For example, the isotropic correction C_i for a Kipp & Zonen CM 121 shadow ring can be calculated from the equation (Kipp & Zonen):

$$C_i = 1/(1 - \frac{2V}{\pi} \cos\delta_s (U_0 \sin l \sin\delta_s + \cos l \cos\delta_s \sin U_0)) \tag{4}$$

where V is the view angle of the shadow ring (in radians), δ_s is the declination of the sun, U_0 is the hour angle at sunset (in radians from solar noon), and l is the latitude. In reality, the sky radiance distribution is not isotropic. The region of the sky near the sun, obstructed by the shadow ring, is brighter than the sky on the average. Therefore, the isotropically corrected diffuse irradiance has to be further corrected with an anisotropic correction factor. A new anisotropic correction method for the horizontal diffuse irradiance measurements, based on a realistic sky radiance distribution model, is presented in publication **II**. In case of a Kipp & Zonen CM 121 shadow ring ($V = 0.185$), the total correction factor C_t can be calculated from the following equation (publication **II**):

$$C_t = 1/(1 - \frac{V \cos\delta_s \int_{-U_0}^{U_0} R_p(\theta_p, \varphi_p)(\sin l \sin\delta_s + \cos l \cos\delta_s \cos U)\, dU}{\int_{0}^{\pi/2} \int_{-\pi}^{\pi} R_p(\theta_p, \varphi_p) \cos\theta_p \sin\theta_p\, d\theta_p\, d\varphi_p}) \tag{5}$$

where R_p is the radiance at point P of the sky, θ_p is the altitude angle of point P, φ_p is the azimuth angle of point P, and U is the hour angle of the sun (in radians from solar noon). As an example, the monthly average correction factors for three Finnish Meteorological Institute sites are presented in Table 2 (publication **I**). The averages in Table 2 are weighted with the irradiances.

Table 2. The monthly averages of isotropic (C_i, eqn 4), anisotropic ($C_a = C_t / C_i$), and total (C_t, eqn 5) shadow ring correction factors for the horizontal diffuse irradiance in Helsinki-Vantaa (1972-93), Jyväskylä and Sodankylä (1971-93); C_t is calculated with the Perez all-weather sky model (Perez & al., 1999a; 1993b)

	Helsinki-Vantaa			Jyväskylä			Sodankylä		
Month	C_i	C_a	C_t	C_i	C_a	C_t	C_i	C_a	C_t
Jan	1.01	1.04	1.06	1.01	1.03	1.03	1.00	1.00	1.00
Feb	1.03	1.07	1.11	1.02	1.06	1.08	1.02	1.04	1.06
Mar	1.07	1.09	1.16	1.06	1.07	1.13	1.05	1.06	1.11
Apr	1.13	1.09	1.23	1.10	1.07	1.18	1.09	1.08	1.17
May	1.17	1.09	1.28	1.14	1.08	1.22	1.13	1.07	1.21
Jun	1.19	1.09	1.29	1.15	1.07	1.23	1.16	1.06	1.23
Jul	1.18	1.09	1.28	1.15	1.07	1.23	1.15	1.07	1.22
Aug	1.15	1.09	1.25	1.12	1.07	1.20	1.11	1.07	1.19
Sep	1.10	1.09	1.20	1.07	1.08	1.16	1.06	1.07	1.14
Oct	1.05	1.08	1.13	1.03	1.06	1.09	1.03	1.05	1.08
Nov	1.02	1.05	1.07	1.01	1.04	1.04	1.02	1.02	1.04
Dec	1.01	1.03	1.04	1.00	1.01	1.02	1.00	1.00	1.00
Ave	1.14	1.09	1.24	1.11	1.07	1.19	1.11	1.07	1.19

As can be seen from Table 2, the correction factors are larger for Helsinki than for the other locations. This is due to the wider shadow ring used in Helsinki for the measurements. The monthly variations in the isotropic correction factor are great, due to the change in the declination of the sun. The average total correction factor is almost 1.30 during the summer in Helsinki, but only about 1.05 around the winter solstice. The anisotropic correction factor is fairly constant, about 1.09, from March to October.

To get an overview of the importance of the shadow ring correction, the yearly average correction (in % of the uncorrected diffuse irradiance) for various correction methods is presented in Fig. 3. In addition to the isotropic correction method (eqn 4), the total correction for eqn (5) calculated with two different sky models, the Brunger sky radiance model (Brunger & Hooper, 1993) and the Perez all-weather sky model (Perez & al., 1993a; 1993b), is presented together with the correction for an earlier anisotropic method (LeBaron & al., 1990). It can be seen that there is no difference between the Brunger and Perez all-weather models, i.e., eqn (5) gives similar results for different sky models that are use to calculate the sky radiance R_p in eqn (5), provided that accurate sky models (publication **IV**) are used. However, the simpler LeBaron method gives a significantly lower average correction than eqn (5). It can be concluded that proper correction of the diffuse irradiance measurements is vital to the correctness of the input data used in the daylight simulation model. Neglecting the correction could lead to an average underestimation of up to 19% of the diffuse solar component.
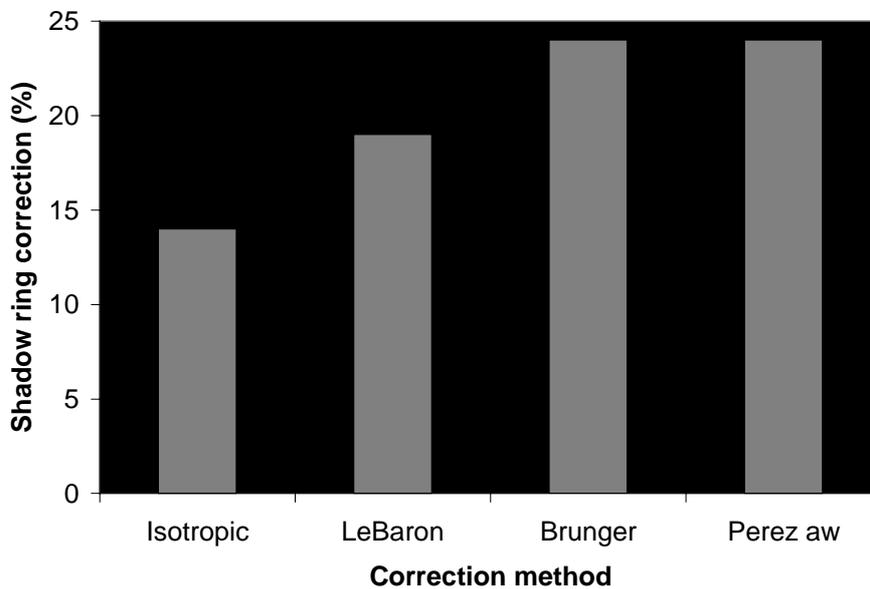

Fig. 3. The yearly average shadow ring correction (%) for the horizontal diffuse irradiance in Helsinki, Finland, 1979, for the different correction methods.

2.3 Luminous efficacy models

The horizontal illuminance values required as input for the daylight simulation tool can be calculated from the irradiance measurements by a luminous efficacy model. The luminous efficacy K is defined as the ratio of the luminous flux and the radiant flux:

$$K = \frac{E}{G} = \frac{K_m \int\limits_{380}^{780} G_\lambda V_\lambda d\lambda}{\int G_\lambda d\lambda} \qquad (6)$$

where E is the illuminance, G is the irradiance, G_λ is the spectral irradiance, V_λ is the spectral sensitivity of the eye, λ is the wavelength, and $K_m = 683$ lm/W is the luminous efficacy constant for photopic (daytime) vision. The notation used above differs slightly from the standard SFS-IEC 50-845 (Suomen Standardisoimisliitto, 1992) but is in line with the publications of this thesis. For monochromatic light with a wavelength of 555 nm, the luminous efficacy K would be 683 lm/W. However, the solar radiation is not monochromatic, and the luminous efficacy of the extraterrestrial solar radiation, for example, is 97.8 lm/W (Littlefair, 1985). The luminous efficacy of daylight is greater than that of typical electric incandescent (15 lm/W) and fluorescent (80 lm/W) light.

The luminous efficacy of global radiation depends mainly on the atmospheric absorption. The atmospheric absorption increases with the distance travelled by light in the atmosphere. Because the atmosphere normally absorbs more infrared radiation than visible light, the luminous efficacy on the earth is higher than outside the earth's atmosphere. However, the luminous efficacy can vary greatly depending on insolation and weather conditions. A detailed description of atmospheric absorption and scattering processes affecting the luminous efficacy of daylight can be found in publication **I**.

One of the first studies on luminous efficacy was carried out by Harald Lunelund in Helsinki, Finland, at the end of 1920's. From the measurements made by Lunelund during 1928-35, Gunnar Pleijel (1954) calculated the yearly average luminous efficacy which was 112 lm/W for the horizontal global radiation. Littlefair (1985) made a thorough literature review of the luminous efficacy measurements made during 1955-1984. In most studies, the global luminous efficacy was between 100 and 115 lm/W. For example, in the measurements of Gillette and Treado (1985) in Maryland, USA, during 1980-83, the average horizontal global luminous efficacy was 107 ± 7 lm/W.

During the past decades, several luminous efficacy models based on simultaneous illuminance and irradiance measurements have been developed. In publication **III**, the

predictions for models of Littlefair (1988), Perez & al. (1990), Olseth and Skartveit (1989), Chung (1992), and Muneer and Kinghorn (1998) were compared with measured luminous efficacies in Otaniemi, Finland (60°11'N, 24°50'E). In addition to these models, a constant luminous efficacy model was included in the comparison. The yearly average of the measured horizontal global luminous efficacy of 110.0 lm/W was used as the constant.

The yearly average horizontal beam (K_b), diffuse (K_d), and global (K) luminous efficacy, relative mean bias difference (*MBD*), and root mean square difference (*RMSD*) for the different luminous efficacy models is presented in Table 3 (publication **III**). The averages are weighted with the measured horizontal global irradiances. As is obvious, the constant model has a zero *MBD* as the measured average was used as the constant. Of the other models, the Olseth & Skartveit model and the Perez model have very low *MBD*s. These two models also have a lower *RMSD* than the constant model, with the Perez model having clearly the lowest *RMSD*. The Littlefair and the Chung models slightly underestimate the luminous efficacy, whereas the Muneer and Kinghorn model overestimates it by about 4%. However, all tested models have an *RMSD* within 2 percentage points (% points) of the *RMSD* of the constant model.

Table 3. The yearly average horizontal beam (K_b), diffuse (K_d), and global (K) luminous efficacy, relative mean bias difference *(MBD)*, and relative root mean square difference (*RMSD*) for the different luminous efficacy models, Otaniemi (60°11'N, 24°50'E), 1996

Model	K_b lm/W	K_d lm/W	K lm/W	MBD %	RMSD %
Constant (measured average)	110.0	110.0	110.0	0.0	8.3
Littlefair	88.4	129.7	108.2	-1.6	10.4
Perez & al.	93.7	126.5	109.4	-0.6	6.7
Olseth & Skartveit	101.4	118.5	109.6	-0.4	8.0
Chung	92.9	122.7	107.2	-2.6	9.6
Muneer and Kinghorn	105.7	124.7	114.8	4.3	9.4

Although the average calculated global luminous efficacy was fairly close to the measured average for all models, there are considerable differences between the diffuse luminous efficacies. Using a constant of 110 lm/W could underestimate the diffuse illuminance by 13%, compared with the Perez model. It can be concluded that the global

constant model is not accurate enough, even though the constant were known beforehand. To get an overview of the relative potential of the beam and diffuse daylight components, the monthly average beam, diffuse, and global horizontal illuminances in Helsinki, calculated with the Perez luminous efficacy model, are presented in Table 4. It can be seen that the yearly average diffuse illuminance is almost 60% higher than the average beam illuminance.

Table 4. The monthly hourly average horizontal beam (E_b), diffuse (E_d), and global (E) horizontal illuminances in Helsinki-Vantaa airport (60°19'N, 24°58'E), 1972-93, calculated from the measured irradiances (publication **I**, Table 3) and the calculated luminous efficacies with the Perez model from the measurements in Otaniemi (60°11'N, 24°50'E), 1996 (publication **I**, Table 11); the averages are calculated over 24 hrs per day

Month	E_b lx	E_d lx	E lx
January	200	1000	1200
February	1000	2900	3900
March	3000	6000	9000
April	6200	9800	16000
May	11300	13200	24500
June	11600	15100	26700
July	9900	14800	24700
August	6600	12900	19500
September	3400	7200	10600
October	1300	3300	4600
November	200	1100	1300
December	100	600	700
Average	4600	7300	11900

2.4 Sky luminance models

Sky luminance L is defined as the amount of luminous flux emitted by an infinitesimal area, at a certain point in the sky and in a certain direction, per unit of solid angle, and per the projection of the receiving area perpendicular to the direction of the light, i.e.

$$L = \frac{d^2\Phi}{d\omega dA \cos\theta_i} = \frac{dE}{d\omega \cos\theta_i} = \frac{dI}{dA \cos\theta_i} \qquad (7)$$

where L is the luminance of the emitting surface, Φ is the luminous flux, ω is the solid angle of the receiving surface, A is the area of the receiving surface, θ_i is the angle of incidence on the surface, E is the illuminance, and I is the luminous intensity.

The luminance value of each point of the sky can be generated by a sky luminance model from the horizontal beam and diffuse illuminance values. The simplest sky model is the isotropic model which assumes that the sky luminance distribution is uniform over the whole sky dome. However, in reality, the circumsolar area and the horizon are brighter than the sky on average (publication **IV**), and this anisotropy should be taken into account in the sky luminance model. In the past, several anisotropic sky models have been developed which use the horizontal illuminance values as input data. In publication **IV**, the CIE clear/overcast model (Littlefair, 1994), the Perraudeau model (CEC, 1993), the Perez-CIE model (Perez & al., 1990), the Perez all-weather model (Perez & al., 1993a; 1993b), and the Littlefair model (Littlefair, 1994) are compared with year-round irradiance measurements at 24 inclined surface orientations. The isotropic sky model and the radiance model of Brunger and Hooper (1993) are also included in the comparison. The radiance and luminance distributions of the sky are not necessarily very different, as was shown in the comparison of publication **IV**. The illuminance on an inclined surface E_{di} can be calculated by the equation (publication **IV**)

$$E_{di} = E_d \frac{\displaystyle\int_{-\pi}^{\pi}\int_{\theta_0}^{\pi/2} L_p(\theta_p,\varphi)\cos\theta_p(\sin\theta_p\cos\beta + \cos\theta_p\sin\beta\cos\varphi)d\varphi d\theta_p}{\displaystyle\int_{-\pi}^{\pi}\int_{0}^{\pi/2} L_p(\theta_p,\varphi_p)\cos\theta_p\sin\theta_p d\varphi_p d\theta_p} \qquad (8)$$

where E_d is the horizontal diffuse illuminance, L_p is the luminance of point P of the sky calculated by the sky model, θ_p is the altitude angle of point P, φ_p is the azimuth angle of point P, β is the inclination angle of the surface, φ is the azimuth angle of point P relative to the normal of the surface, and $\theta_0 = 0$, when $-\pi/2 \leq \varphi_p \leq \pi/2$, and

$$\theta_0 = \arctan(-\tan\beta\cos\varphi) \text{ otherwise.} \qquad (9)$$

The irradiance on the inclined surface G_{di} can be calculated instead of the illuminance E_{di} by replacing E_d by the horizontal diffuse irradiance G_d and L_p by the radiance R_p in eqn (8). As can be seen, the units in the integrals of eqn (8) cancel out each other - the denominator is merely a normalizing factor corresponding to the measured horizontal diffuse irradiance, as the integrals are calculated numerically. The average *MBD* and *RMSD* values of all the surface orientations for all sky distribution models are presented in Table 5 (publication **IV**).

Table 5. The average *MBD* and the *RMSD* (as % of the measured average) of all 24 surface orientations for the different sky distribution models, Isotr = isotropic, Cl/Oc = CIE clear/overcast, Perra = Perradeau, P-CIE = Perez-CIE, PerAW = Perez all-weather, Littl = Littlefair sky luminance model, and Brung = Brunger sky radiance model

	Isotr	Cl/Oc	Perra	P-CIE	PerAW	Littl	Brung
MBD	-1.5	-1.9	1.0	-2.7	-2.1	-3.2	-4.0
RMSD	23.6	13.3	14.5	12.0	11.1	11.9	12.5

As can be seen, the average *MBD* of all surface orientations is relatively low for all models. However, the *RMSD* of the isotropic model is clearly higher for the isotropic than for the other models. The large biases for the different surface orientations for the isotropic model cancel out each other in the average *MBD*. For example, the isotropic model underestimates the irradiance on a vertical south-facing surface by 12.5% on the average (publication **IV**). The best model seems to be the Perez all-weather model which has the lowest *RMSD* for 18 of the 24 surface orientations (publication **IV**).

The comparisons presented above are based on the measurements of the total irradiances (including the beam, the diffuse, and the reflected component). To get an overview of the effect of the sky distribution model on the diffuse component, the annual diffuse irradiation on various vertical surfaces in Helsinki has been calculated in Table 6 (publication **I**). As can be seen, the isotropic model could underestimate the annual diffuse irradiation by 26% in the south and overestimate it by 27% in the north, compared with the Perez all-weather model. For this reason, it is important that realistic, anisotropic sky distribution models are used in the daylight calculations.

Table 6. Annual diffuse irradiation (in kWh/m^2) on south-, west-, east-, and north-oriented vertical surfaces for different sky models, Helsinki-Vantaa, 1979

Sky model	South	West	East	North
Isotropic	248.9	248.9	248.9	248.9
CIE clear/overcast	311.5	275.7	263.5	214.9
Perraudeau	352.9	305.4	293.3	232.1
Perez-CIE	355.2	281.7	269.5	186.9
Perez all-weather	335.0	276.8	267.6	195.7
Littlefair	331.0	278.6	262.0	190.2
Brunger radiance	315.4	263.7	253.2	190.4

2.5 Summary of the daylight calculation measures

To summarize the importance of the various steps in daylight modelling, the yearly average error induced by using simple methods compared with the best solutions found in publications **II-IV** is presented in Table 7. It can be concluded that using uncorrected input irradiance measurements with constant luminous efficacy and isotropic sky luminance model results in underestimating the daylighting potential by almost a half for a southern orientation in Helsinki. In this thesis, the aim has been to minimize these errors through the improved modelling approaches presented in publications **II-IV**.

Table 7. The yearly average error induced by using simple daylight calculation measures compared with the best solutions in publications **II-IV**, Helsinki, south, 1979

II Neglecting the shadow ring correction	-19%
III Using constant luminous efficacy	-13%
IV Using isotropic sky model	-26%
Total error of measures **II-IV**	-48%

3 DAYLIGHT SIMULATION TOOL DeLight

A schematic diagram of the DeLight daylight simulation tool was presented in Fig. 2 in section 1. It is possible to use any of the luminous efficacy and sky luminance models introduced in section 2 with DeLight. However, the best models found in the comparisons (publications **III** and **IV**) with the measurements have been used in the calculations of this thesis: the Perez luminous efficacy model (Perez & al., 1990) and the Perez all-weather sky luminance model (Perez & al., 1993a; 1993b). The interior light transfer model of DeLight is briefly described in section 3.1, the simulation method in section 3.2, and model verification in section 3.3.

3.1 Interior light transfer model

The interior horizontal total daylight illuminance E_r at a point R is the sum of three components: the beam $E_{r,b}$, the diffuse $E_{r,d}$, and the reflected illuminance $E_{r,r}$, i.e.,

$$E_r = E_{r,b} + E_{r,d} + E_{r,r}. \tag{10}$$

The calculation of the beam illuminance is relatively straightforward if the position of the sun and the room geometry are known. If the sun is visible at the interior point R, the interior horizontal beam illuminance $E_{r,b}$ is given by

$$E_{r,b} = \tau_w(\theta_i) \, K_b \, G_b \,, \tag{11}$$

where $\tau_w(\theta_i)$ is the window light transmittance at the angle of incidence θ_i, K_b is the beam luminous efficacy, and G_b is the outdoor horizontal beam irradiance. The window light transmittance is given by the approximation of Rivero (Bryan and Clear, 1981):

$$\tau_w(\theta_i) = 1.018 \, \tau_w(0) \cos \theta_i \, (1 + \sin^3\theta_i) \,, \tag{12}$$

where $\tau_w(0)$ is the window light transmittance with the angle of incidence $\theta_i = 0$, and the angle of incidence is calculated from the equation

$$\cos\theta_i = \cos \theta_s \cos (\varphi_s - \varphi_w) \,, \tag{13}$$

where θ_s is the solar elevation, φ_s is the solar azimuth angle, and φ_w is the azimuth angle of the window normal.

The interior horizontal diffuse illuminance $E_{r,d}$ is given by (publications **I** and **V**)

$$E_{r,d} = \int_0^{w_w}\int_0^{h_w} \frac{\tau_w Lzy\,dx\,dy}{(x^2+y^2+z^2)^2} = \frac{\tau_w L}{2}\{\frac{z}{\sqrt{h_r^2+z^2}}(\arctan\frac{x_w+w_w-x_r}{\sqrt{h_r^2+z^2}}+\arctan\frac{x_r-x_w}{\sqrt{h_r^2+z^2}})$$

$$-\frac{z}{\sqrt{(h_r+h_w)^2+z^2}}(\arctan\frac{x_w+w_w-x_r}{\sqrt{(h_r+h_w)^2+z^2}}+\arctan\frac{x_r-x_w}{\sqrt{(h_r+h_w)^2+z^2}})\}, \qquad (14)$$

where L is the luminance at the centre of the part of the sky visible to point R (calculated by the sky luminance model), z is the horizontal distance between the window and point R, h_r is the vertical distance between the lower edge of the window and point R, w_w is the width of the window, h_w is the height of the window, x_w is the horizontal distance between the left wall and the left edge of the window, and x_r is the horizontal distance between the left wall and point R. The room geometry is illustrated in Fig. 4.
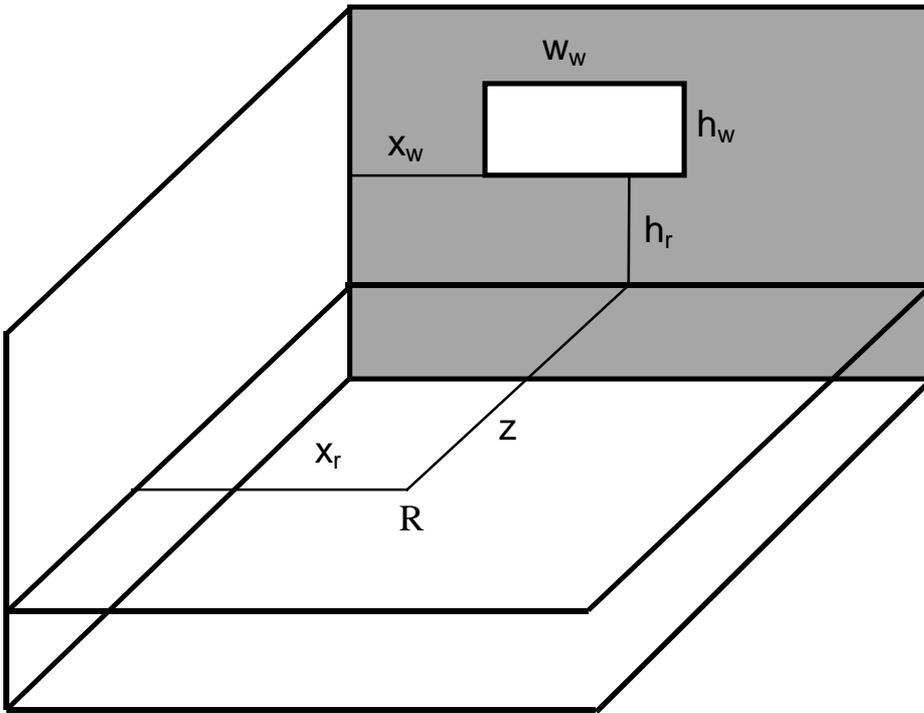

Fig 4. The room geometry for calculating the interior horizontal diffuse illuminance.

The reflected daylight component is the most complicated one to simulate. It is possible to formulate similar expressions as eqn (14) to all interior surfaces (publication **I**). When the beam and diffuse daylight illuminance on the ceiling and the walls has been determined, the reflected illuminance on the horizontal surface can be calculated. However, taking into account all the multiple interior reflections would dramatically increase the computation time. In DeLight, only the exterior reflections from the ground and first order interior reflections are calculated. This will lead to a slight underestimation of the reflected component, but as shown in publications **I** and **V**, this error is not significant to the daylight availability calculations.

3.2 Description of the simulation method

The calculation of eqn (14) and similar equations for other interior surfaces is not possible analytically for the entire surface of interest, and therefore, the illuminance must be calculated at selected points on the surface. Usually, we are interested in the illuminance on the horizontal desk level. In DeLight, all the interior room surfaces can be divided into smaller parts (Fig. 5) and the illuminance is calculated at the centre of each part. Possible exterior obstructions are taken into account in the calculations.
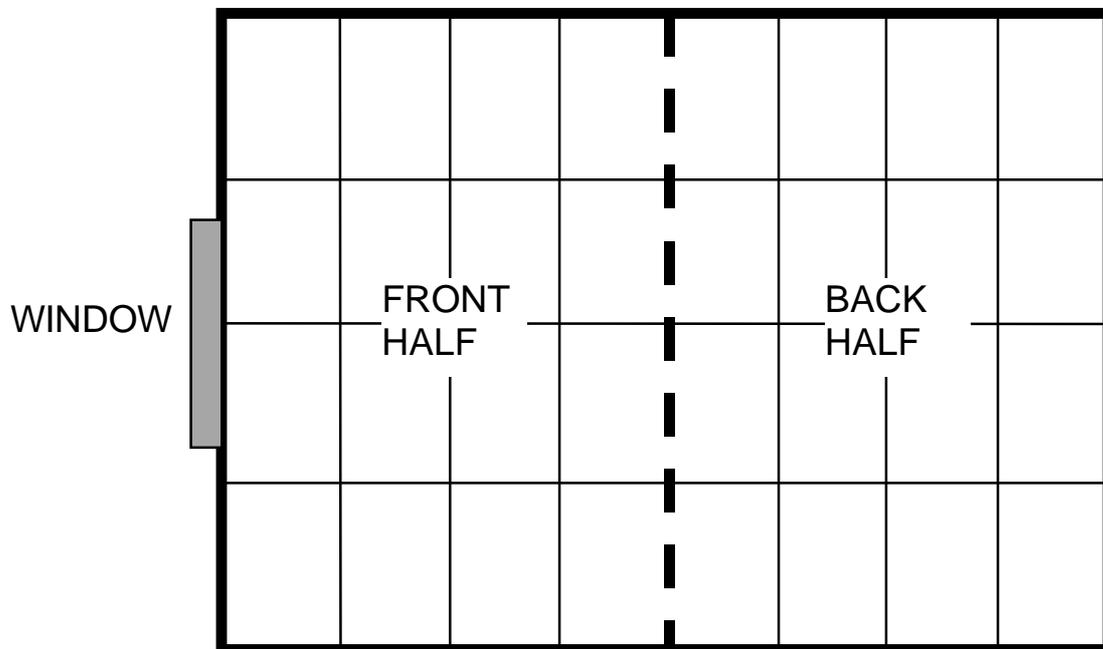
Fig. 5. The division of the room into a front and a back half with subsections to improve the calculation resolution.

The interior horizontal diffuse illuminance drops very rapidly with the distance from the window: for a typical office room, the diffuse illuminance at the centre of the room is only a quarter of that near the window (Vartiainen, 1996). Therefore, it is not sufficient to calculate the daylight illuminance only at one point of the room. For this reason, the room is divided into two equal zones: the front half closest to the window and the back half (Fig. 5). Both halves can be further divided into subsections to improve the calculation resolution. The average illuminance of both halves is calculated for each hour. In both halves, the hourly illuminance up to the recommended working plane illuminance level is counted as useful daylight. Illuminance exceeding this level is counted as surplus daylight, and illuminance short of this level must be supplemented by electric lighting.

3.3 Model verification

To verify the daylight simulation model DeLight, horizontal illuminances at three points in a test room were measured simultaneously with the horizontal global and the diffuse irradiance over the year 1996 at Helsinki University of Technology, Otaniemi, Finland (60°11'N, 24°50'E). Kipp & Zonen CM 11 pyranometers with spectral selectivity of ±2% and tilt response of ±0.25%, together with a CM 121 shadow ring, were used for the irradiance measurements. The illuminances were measured inside a test room whose depth was 4.7 m, width 4.0 m, and height 3.0 m. The window of the room was oriented to the southwest (the azimuth angle of the window normal was 60°). The effective width of the window glazing was 1.95 m and the height 1.15 m. The lower edge of the window was 0.4 m higher than the reference plane which was 0.75 m from the floor. The interior horizontal illuminance was measured at a distance of 1.35 m (#1, front), 2.65 m (#2, middle), and 3.95 m (#3, back) from the window (Fig. 6). The reflectances of the interior surfaces were 0.7 for the ceiling and the right wall, 0.5 for the left and the back walls, and 0.3 for the floor (Vartiainen, 1996). There were no significant obstructions on the horizon of the measurement points. YF-1065A photometers with 4% accuracy were used. One of the photometers was calibrated at the Finnish National Standards Laboratory for optical quantities, and the other photometers were compared to this one.

The measured horizontal interior illuminances were compared with the values computed by the simulation program DeLight from the measured hourly irradiances, and the annual mean bias relative differences (*MBRD*) and root mean square relative differences (*RMSRD*) of the computed values were calculated. Only the hours when the sun was above the horizon and both the measured and the computed illuminance values exceeded 1 lx are included in the comparison (Table 8a). However, the illuminance values exceeding the recommended working plane illuminance level have no effect on

the annual auxiliary electricity requirement. Therefore, the comparison has also been made for the measured illuminance values up to 500 lx (Table 8b) and 300 lx (Table 8c). In other words, the hourly error was zero when the measured illuminance exceeded 500 lx in Table 8b and 300 lx in Table 8c.
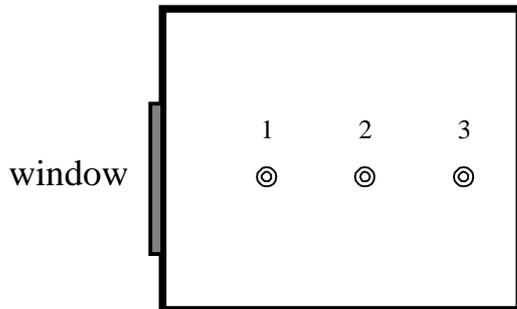

Fig. 6. The positioning of the photometers in the verification measurements of DeLight in a test room: 1 - front, 2 - middle, and 3 - back of the room.

Table 8. The annual mean bias relative differences *(MBRD)* and root mean square relative differences (*RMSRD*) of the computed illuminances (%) in Otaniemi, 1996, for the measured a) total illuminance, b) the illuminance up to 500 lx, and c) up to 300 lx

Illuminance	Front of the room		Middle of the room		Back of the room	
	MBRD	*RMSRD*	*MBRD*	*RMSRD*	*MBRD*	*RMSRD*
a) Total	-3.7	23.7	-6.5	26.7	-11.3	30.6
b) Up to 500 lx	0.2	15.3	-0.9	20.8	-5.8	25.7
c) Up to 300 lx	0.6	13.5	0.2	19.5	-3.5	23.9

As can be seen from Table 8, the simulation model underestimates the measured illuminance by about 4-11% which is partly due to the inaccuracies in the treatment of the reflected beam light. Only first order interior reflections are included in the model. Therefore, the computed illuminance values are naturally lower than the measured values. Also, the errors are greater further away from the window. The error is greatest at the back of the room since the portion of the reflected light is greatest there. Moreover, all reflections are assumed to be totally isotropic which is a simplification of the real situation. However, the annual *MBRD*s are within the accuracy of the photometers (± 4%) if only the hours when the measured illuminance was less than 300

lx are taken into account. The accuracy of the model would be worse in a room with very high interior reflectances. The reflectance of the floor is not as significant as the other interior surfaces because the daylight entering the room floor must be reflected at least twice before it can reach the desk level (publication **V**).

To exclude the inaccuracy caused by the beam radiation, an independent set of measurements was used to verify the simulation model under overcast conditions (publication **I**). 29 days of the period from April to November 1995 were selected for the comparison. Only totally overcast days or days when no beam sunlight entered the room were chosen. Apart from the measurement point at the back of the room, the *MBRD* for the overcast days was within the accuracy of the photometers. At the back of the room, the *MBRD* was only -5.6% and the *RMSRD* 16.4%.

It can be concluded that the simulation tool DeLight models the interior illuminance within ±6% accuracy under overcast conditions or with illuminances up to 500 lx. The accuracy is reduced when beam sunlight enters the room. However, this is not critical to the useful daylight fraction, as most of the beam illuminance is usually in excess of the recommended illuminance level. For example, if the lighting requirement were 500 lx for the front half and 300 lx for the back half of the room, the error on the yearly auxiliary electricity requirement would be just about 2%. Therefore, to calculate the auxiliary lighting electricity requirement, it is far more important to be able to model accurately the conditions when daylight alone is not sufficient.

In addition to the relatively good accuracy of the simulation tool DeLight, its greatest advantage is its speed. The simulation of all working hours of the day takes only a few minutes with a common pentium PC. As an example of the more complicated models, the corresponding simulation time for Radiance (University of California, 1993) with a realistic sky model and reasonable number of multiple reflections is several days (Arpiainen, 1999). In solar facade optimization calculations with numerous simulation runs, the program execution time is a critical factor.

A comparison of DeLight and Radiance simulation tools with the measurements is presented in Table 9 (publication **I**; Arpiainen, 1999) for February and September 1996 in the same test room as described earlier. As can be seen from the table, DeLight performed slightly better than Radiance, especially in February. Generally, both models had greater errors under sunny conditions than under overcast conditions (Arpiainen, 1999). Because of its relatively good accuracy and fast computation speed, the simulation tool DeLight has been used in all the subsequent daylight calculations of this thesis.

Table 9. The monthly mean bias relative difference *(MBRD)* and root mean square relative difference (*RMSRD*) between the computed and measured illuminances (in %) in Otaniemi (60°11'N, 24°50'E), for DeLight and Radiance simulation tools in February and September, 1996

Month, model	Front of the room		Middle of the room		Back of the room	
	MBRD	*RMSRD*	*MBRD*	*RMSRD*	*MBRD*	*RMSRD*
Feb, DeLight	-8.1	20.1	-1.7	20.7	-4.0	21.7
Feb, Radiance	-18.3	24.8	-16.7	26.2	-13.9	28.7
Sep, DeLight	-13.7	22.0	-15.4	25.9	-22.4	30.0
Sep, Radiance	-17.6	25.0	-14.5	26.2	-10.1	30.3

4 DAYLIGHT AVAILABILTY WITH SOLAR FACADES

The main aim of this thesis has been to optimize the daylight utilization and assess the subsequent lighting electricity savings in buildings with solar facades. With the DeLight simulation tool, it is possible to make such calculations. In this section, the various parameters affecting the daylight availability are analysed, e.g.:

- location
- orientation of the facade
- shading system
- window glazing area
- position and shape of the window
- hours of lighting requirement
- lighting requirement level
- electric light control strategy

In section 5, the electricity benefits of daylight in solar photovoltaic facades are analysed. It must be emphasized that the results of this section apply also to conventional facades having traditional windows but no other solar components.

4.1 Input data for the daylight simulations - reference case

The main input parameters for the daylight simulations analysed in this section are presented in Table 10. All the simulations are made for four locations: Trapani, Sicily (37°55'N, 12°30'E), Paris, France (48°46'N, 2°1'E), Helsinki, Finland (60°19'N, 24°58'E), and Sodankylä, Finland (67°22'N, 26°39'E). Hourly irradiance measurements from Test Reference Years have been used as input data for all locations. The input data presented in Table 10 are used for the basic room case simulations where the window glazing area is 24% of the total facade area. Moreover, the illuminance requirement is 500 lx for the front half of the room and 300 lx for the back half. It is assumed that the tasks requiring more accurate vision could be performed in the front half of the room. These illuminance requirements correspond to the normal office work recommendations in various countries (CIBSE, 1984; Suomen Valoteknillinen Seura, 1986; IESNA 1993).

Table 10. The main input parameters of the daylight simulations

Luminous efficacy model	Perez
Sky luminance model	Perez all-weather
Sky segments used in the luminance calculation	16 x 16
Window light transmittance at normal incidence	0.70
Height of the window	1.44 m
Width of the window	1.70 m
Window sill height	1.10 m
Distance from left wall to the window left edge	0.85 m
Reflectance of the walls and the ceiling	0.70
Reflectance of the floor	0.30
Ground reflectance	0.15*
Room depth	5.00 m
Room height	3.00 m
Room width	3.40 m
Room division	8 x (8+4)
Desk level height	0.70 m
Illuminance requirement in the front half of the room	500 lx
Illuminance requirement in the back half of the room	300 lx
Hours of lighting requirement	9 am to 5 pm, 5 days / week
Daylight saving time applied	1st April to 31st October

*) For the Finnish locations, monthly measured average reflectances are used instead

4.2 Shading system for the beam sunlight

The beam sunlight usually causes discomfort glare and more overheating than diffuse skylight, and is, therefore, less wanted. Shading would be needed for southern, western, and eastern facade orientations. For example, Venetian blinds can be used to reflect back the beam sunlight, but let in some of the valuable diffuse daylight. To assess the effect of the shading system on the daylight availability, five different systems have been analysed:

(1) no blinds are used and all the beam and diffuse daylight is allowed into the building;

(2) an ideal system where all the beam sunlight is reflected back but all diffuse daylight is allowed in;

(3) all beam sunlight and 75% of the diffuse daylight is reflected back when beam sunlight would enter the room, otherwise, all diffuse daylight is allowed in;

(4) all beam sunlight and 75% of the diffuse daylight is reflected back when beam sunlight would enter the room, otherwise, 25% of the diffuse daylight is reflected back;

(5) all beam sunlight and all diffuse daylight is reflected back when beam sunlight would enter the room, otherwise, 25% of the diffuse daylight is reflected back.

Advanced shading systems, such as light shelves, were not considered here because they are not supported by the DeLight simulation tool. System (4) is probably the most realistic one because the blinds will also reflect back most of the diffuse daylight in order to block the beam sunlight when the sun would shine in. When the sun is not shining, the blinds can be opened to let in a maximum amount of diffuse light. If the blinds are not lifted up, they will still reflect back some of the diffuse daylight. System (4) could be improved a little by lifting the blinds up when the sun is not shining (system 3) but this would require more interference by the occupants or a more expensive automated blind adjusting system. System (5) is a slight simplification of totally closed Venetian blinds, since in reality, they would let in a small portion of daylight.

The percentages for systems (3-5) are based on the measurements made in Otaniemi, Finland, where the horizontal daylight illuminance, when the blinds where applied to block beam sunlight, ranged from 20% in winter to 30% in summer in the front, and from 25% to 50% in the back part of the room, compared with the illuminances without the blinds. When the sun was not shining in, the optimally opened (not lifted up) blinds let in 70-80% in the front, and 75-90% in the back part of the room. Therefore, the diffuse light fraction of 25% for the closed and 75% for the opened blinds was chosen for the automatic system (4) in this study. However, the daylight transmission through the blinds is not constant; it depends e.g. on the solar elevation. Moreover, the adjustment of the blinds is a highly subjective matter, some people would close the blinds more than the others (Bülow-Hübe, 2000; Vine & al., 1998). In the pilot study of Bülow-Hübe (2000), the average measured desk level daylight illuminance in the front part of the room with 50 subjects was 22% when they had adjusted the blinds, compared with the illuminance immediately before the adjustment when the blinds were lifted up. Moreover, a completely automated system was less preferred by 12 of 14 subjects than an auto user control system in a study (Vine & al., 1998) where the subjects were able to adjust the blinds and the electric light level.

For the above reasons, the actual energy savings of daylight in real offices with differently behaving occupants are very difficult to predict, and therefore, simplified constant diffuse daylight fractions for closed (25%) and opened (75%) blinds are assumed here. For all systems except (1), either manual or automated adjusting of the blinds according to the insolation conditions, with the stated diffuse daylight fractions, is assumed.

With all systems, a continuous electric light dimming control system would be required to utilize the full daylighting potential. Fully automated shading and light control systems are currently coming to the market; a prototype has been tested in the USA (Lee & al., 1998). An ideal continuous electric light control system is assumed in the following simulations, unless stated otherwise, because with an on/off control system, a large part of the useful daylight would be wasted (publication **VII**). In each half of the room, there is an independently controlled luminaire and the electric light is adjusted so that the sum of daylight and electric light illuminance is at least at the required level. The yearly average daylight availability *DA* (in % of the lighting requirement during the office hours of the year) for the different shading systems at different facade orientations at four locations with the input parameters of Table 10 is presented in Fig. 7 (publication **I**).

As can be seen from the small difference between systems (1) and (2), the beam sunlight is almost always in excess of the lighting requirement: the *DA* is at most 2% greater when all beam sunlight is taken into account. However, when a realistic shading system (4) is used, almost a third of the valuable diffuse daylight is lost at all locations in the southern facade orientation. For north-oriented facades, the *DA* remains the same since there is no beam sunlight on the northern side during office hours. For east- and west-oriented facades, the *DA* decreases by about a fifth. The effect of lifting the blinds when no beam sunlight would enter the room (system 3) is relatively small, about 1-3 percentage points for south-facing and 5-7% points for east- and west-facing rooms. Closing the blinds completely when beam sunlight is entering the room has a dramatic effect: 70-90% of the valuable diffuse daylight is lost in south-facing rooms and about half in east- and west-facing rooms.

The shading system (4) will be used in the daylight availability calculations of the following sections. System (4) was also used for the daylight calculations in publications **I**, **VI,** and **IX**. The other shading systems have been used by the author in previous publications: system (1) in publication **VIII** and by Vartiainen (1996), system (2) in publication **V**, and system (3) with a different diffuse shading factor in publication **VII**. With systems (1-3), the *DA* is naturally higher, but system (4) probably gives the most realistic estimation of the possible energy savings achieved by daylighting.
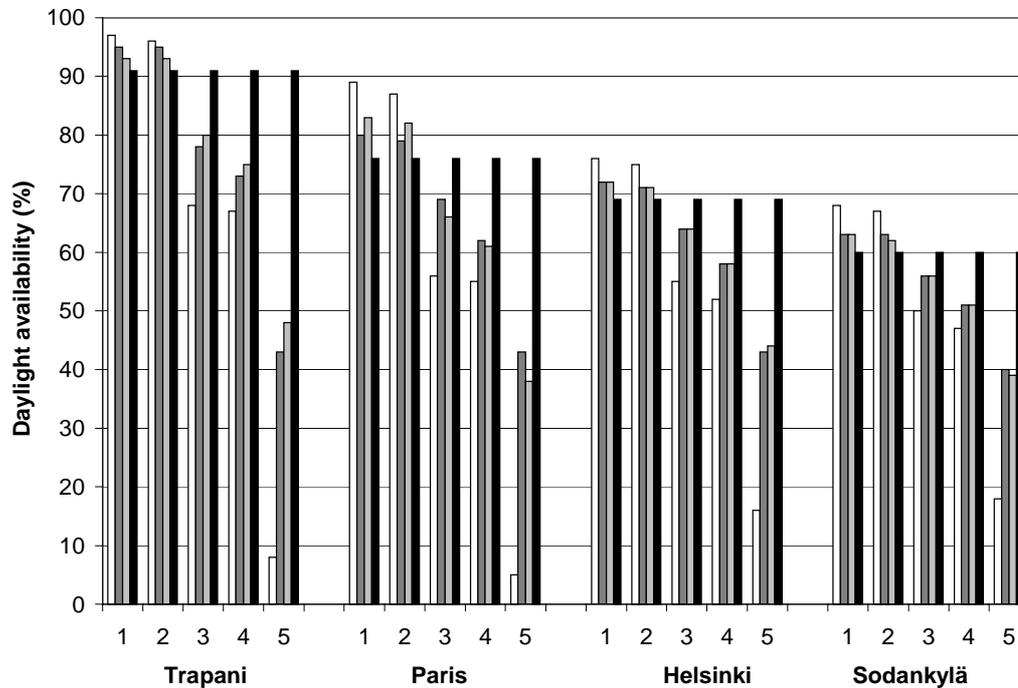
Daylight availability (%)

100
90
80
70
60
50
40
30
20
10
0

1 2 3 4 5   1 2 3 4 5   1 2 3 4 5   1 2 3 4 5

Trapani   **Paris**   **Helsinki**   **Sodankylä**

Fig. 7. The yearly average daylight availability *DA* (% of the lighting requirement during the office hours) at four locations for the different shading systems: (1) without blinds, (2-5) with blinds letting in no beam sunlight and letting in diffuse light (2) 100%, (3) 25% when blinds are closed and 100% when opened, (4) 25% when closed and 75% when opened, (5) 0% when closed and 75% when opened; and for different facade orientations: white = south, dark grey = west, light grey = east, black = north.

4.3 Window area

The effect of window area on the daylight availability is illustrated in Fig. 8 (publication **I**). The *DA* for window areas of 14%, 36%, 48%, 60%, and 72% of the total facade area in addition to the above base case (24%) for different locations and facade orientations is calculated with the shading system (4). As can be seen, decreasing the window area to 14% of the total facade area will decrease the *DA* 13-20% points, depending on the location. Increasing the window area to 36% will increase the *DA* 9-13% points for south-, west-, and east-facing rooms, but only 5-8% points for the north-facing rooms. Increasing the window area to 48% increases the *DA* a further 3-7% points. Increasing the window area beyond 48% does not significantly increase the *DA* for any facade orientation.
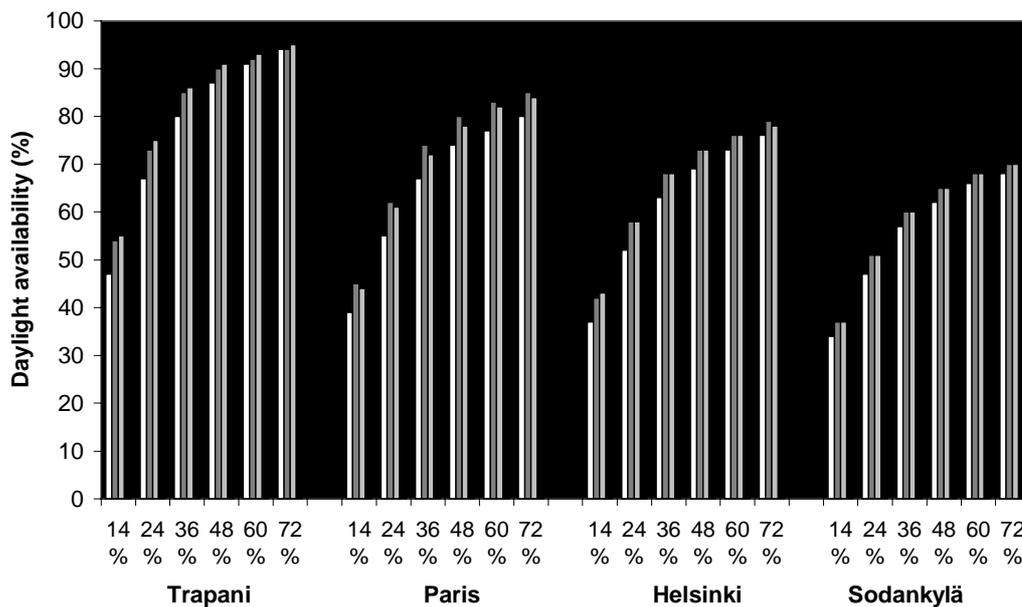
Fig. 8. The yearly average daylight availability *DA* (in % of the lighting requirement during the office hours) for the shading system (4) for the different window areas (in % of the total facade area) at four locations and for different facade orientations: white = south, dark grey = west, light grey = east, black = north.

4.4 Window position and shape

The window position and shape have a relatively small effect on the daylight availability compared with the window area because the diffuse illuminance depends mainly on the solid angle of the window seen at the interior point of the reference (see Fig. 4). For a given window area, the window position and shape have only a little effect on the solid angle of the window. In publication **V**, it was concluded that the optimal shape of the window is close to the shape of the window facade and that the optimal position is near to the centre of the part of the facade above the desk level (Fig. 9). The horizontal position of the window is not as important as the vertical position. Placing the window higher gives a more uniform daylight distribution, i.e., less daylight in the front and more daylight in the back half of the room. However, the overall *DA* of the room does not change much. The yearly average daylight availability for different window sill heights is presented in Table 11 (publication **I**).

As can be seen from the table, the difference between the lowest and the highest *DA* with different window sill heights is only 1-6% points, depending on the location and

the window orientation. Generally, the *DA* is greater for a higher placed window than for a lower placed window, but the window cannot be positioned very high up without sacrificing the outside view of the occupants. On the other hand, it is not sensible to place the window below the desk level because the daylight coming into the room below the desk level has a small effect on the illuminance on the desk level (publication **V**).
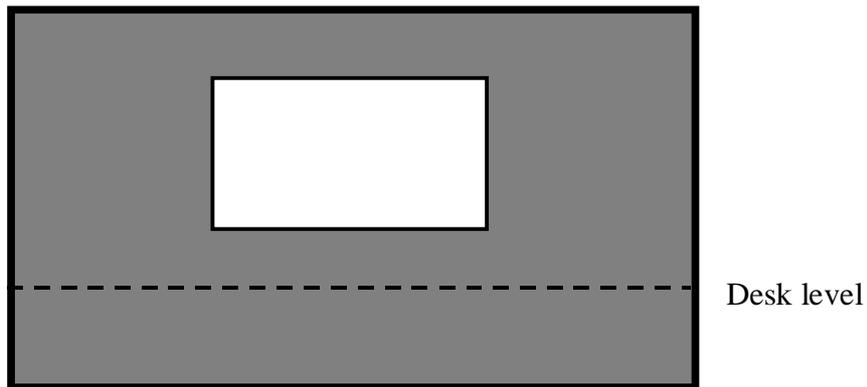

Fig. 9. The optimal position of the window is close to the centre of the part of the facade above the desk level.

Table 11. The yearly average daylight availability *DA* (in % of the lighting requirement during the office hours) for different window sill heights (relative to the desk level height) at four locations and for four window orientations, S = south, W = west, E = east, N = north

Sill height - desk level	Trapani (38°)				Paris (49°)				Helsinki (60°)				Sodankylä (67°)			
	S	W	E	N	S	W	E	N	S	W	E	N	S	W	E	N
0.0 m	66	72	71	89	52	57	58	74	52	54	54	68	46	48	47	59
0.2 m	67	73	72	91	53	58	60	76	52	56	57	69	47	50	50	60
0.4 m	67	73	75	91	55	62	61	76	52	58	58	69	47	51	51	60
0.6 m	68	75	75	91	54	63	61	75	53	59	59	69	47	52	51	60
0.8 m	68	76	75	89	54	63	61	74	54	58	58	68	48	51	51	59

4.5 Hours of lighting requirement

In the previous analysis, it has been assumed that lighting is needed only during the office hours (9-17) of the day. Obviously, the *DA* will decrease if lighting is also required outside the office hours. The *DA* for the following occupancy schedules has been calculated:

(1) midday (12-14)
(2) office hours (9-17)
(3) waking hours (7-23)
(4) all day (0-24)
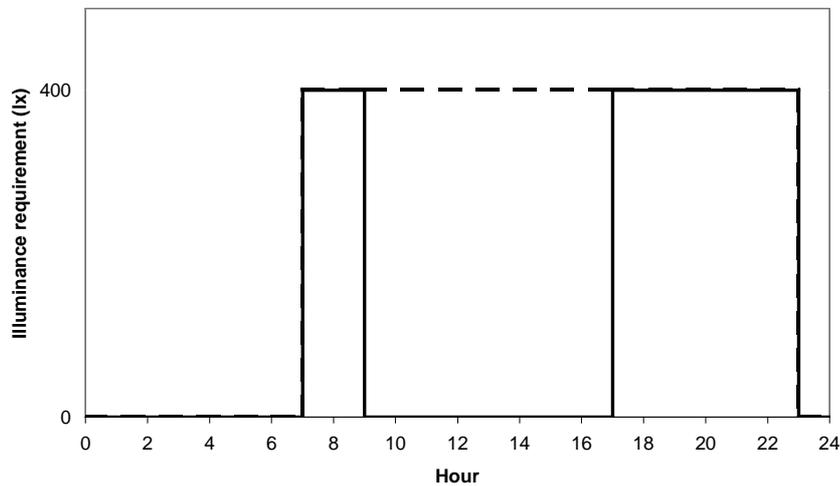(5) domestic (7-9 and 17-23 on workdays, 7-23 on weekends; Fig. 10)

Fig. 10. The average illuminance requirement of the room for the domestic occupancy schedule (5) during workdays (Monday to Friday 7-9 and 17-23, solid line) and weekends (Saturday and Sunday 7-23, dashed line). The 400 lx is an average of the lighting requirements for the front (500 lx) and back (300 lx) half of the room.

The occupancy schedule (1) has been included just to show the maximum daylight availability around solar noon. The yearly average *DA*s for the different occupancy schedules and for different facade orientations at four locations are presented in Fig. 11 (publication **I**). It can be seen that a round-the-clock lighting requirement (0-24) will reduce the *DA* by about one half. For typical waking hours (7-23), the *DA* is 13-29% points less than for office hours. On the other hand, if lighting were needed only during the midday hours, the *DA* would increase 2-18% points. For the domestic occupancy schedule, the *DA* is only slightly higher than for the round-the-clock lighting

requirement because the *DA* for the evening hours (17-23) is only 17-36%, depending on the location and the orientation.
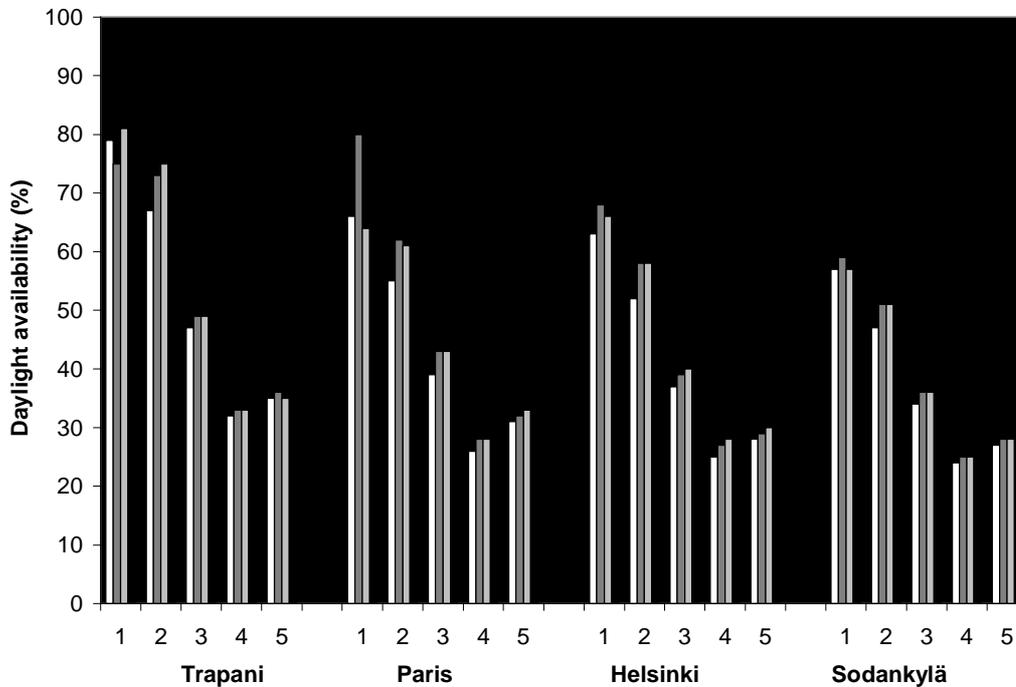

Fig. 11. The yearly average daylight availability *DA* (in % of the lighting requirement during the occupancy hours) for the different occupancy schedules (1 = 12-14, 2 = 9-17, 3 = 7-23, 4 = 0-24, 5 = domestic) at four locations and for different facade orientations: white = south, dark grey = west, light grey = east, black = north.

4.6 Lighting requirement level

The effect of the lux level of the lighting requirement on the *DA* is illustrated in Fig. 12 (publication **I**). For example, if only 100 lx were needed in both room halves, about 97% of the lighting requirement during the office hours could be produced by daylight in Trapani; the *DA* for Paris would be about 90%, for Helsinki about 83%, and for Sodankylä about 73%. These figures are very close to the average proportion of the working day during which there is any daylight available at these locations. The lighting level of 100 lx would be adequate for corridors and areas visited occasionally with visual tasks calling for only limited perception of detail (CIBSE, 1984). On the other hand, if 500 lx were required in both room halves, the *DA* would be 9-16% points less than in the reference case (5) where only 300 lx is needed in the back half of the room.

If only 100 lx were needed in the back half, the *DA* would be 4-15% points higher than in the reference case.
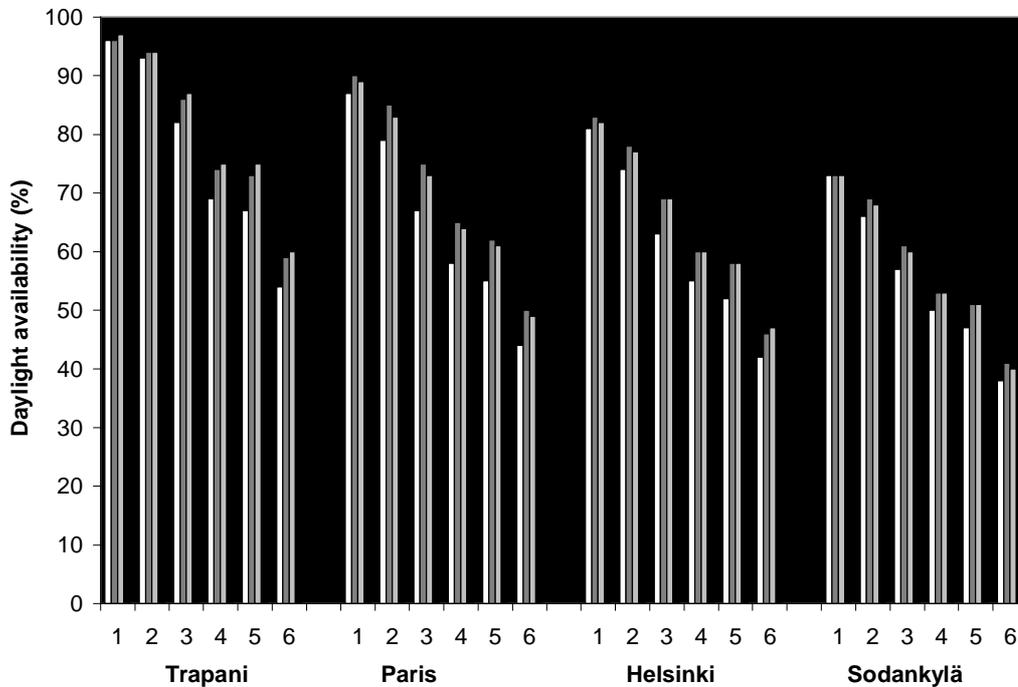

Fig. 12. The yearly average daylight availability *DA* (in % of the lighting requirement during the office hours) for the different lighting requirements (1) $E_{req,f} = E_{req,b} = 100$ lx; (2) $E_{req,f} = 300$ lx, $E_{req,b} = 100$ lx; (3) $E_{req,f} = 500$ lx, $E_{req,b} = 100$ lx; (4) $E_{req,f} = E_{req,b} = 300$ lx; (5) $E_{req,f} = 500$ lx, $E_{req,b} = 300$ lx; (6) $E_{req,f} = E_{req,b} = 500$ lx; at four locations and for four facade orientations: white = south, dark grey = west, light grey = east, black = north.

4.7 Electric light control strategy

The preceding calculated daylight availabilities are based on the assumption that the control system of the electric lighting system permits continuous dimming, i.e., only the illuminance falling short of the required level is provided by electric light. With continuous dimming, the full daylight potential can be utilized. However, in most existing offices, on/off control is used. With on/off control systems, the electric light is always at full power (on) when the daylight illuminance is below the required level. When the daylight illuminance alone is adequate, the electric light is at zero power (off). An ideal transition for switching on/off is assumed, although in reality, the switching off illuminance can be a little higher than the switching on illuminance.

An intermediate option would be an on/half/off control where the electric light can also be at half of the full power. This could be easily implemented since most office luminaires consist of two fluorescent tubes which could be controlled independently.

The *DA* for the different electric light control strategies is presented in Fig. 13 (publication **I**). For the non-continuous control strategies, it is assumed that the electric light can always be switched on/off every hour, depending on the daylight illuminance. It can be seen that with the on/off control strategy at south-, west-, and east-facing rooms, the *DA* is less than half of that with the continuous dimming. This indicates that for most hours, the daylight illuminance is below the required level and must be at least partly supplemented by electric lighting. For north-facing rooms, the *DA* with on/off control does not decrease as dramatically, since during the majority of the working hours when daylight is available, the daylight illuminance exceeds the required level. This is due to the fact that no blinds are needed on north-facing windows and valuable diffuse daylight is not lost when the sun is shining. With the on/half/off control strategy, the *DA* is only 9-21% points less than with the continuous control, depending on the location and the window orientation, because full power is not always needed when the daylight illuminance is below the required level.

The calculated *DA*s for the on/off control strategy are probably closest to the realistic daylight availabilities achieved in existing buildings. If electric light is switched on/off manually by the occupants, the results could be even too optimistic since it is unlikely that every occupant is always going to switch off the electric light every hour when the daylight illuminance is sufficient. Moreover, it was assumed that the blinds were also adjusted every hour according to the sunlight which also requires intervention by the occupants, or automated blind control.

In real cases, the occupants might leave the blinds closed when it is not necessary any more. For example, it is possible that the electric lights are switched on/off and the blinds are adjusted only three or four times during the day: in the morning, during the lunch hour, and in the evening when leaving the office. That way, about half of the useful daylight would be lost (publication **VII**). Therefore, it is obvious that a mere on/off control of electric lighting is not enough for optimal use of daylight. Full daylight utilization would necessitate an intelligent daylight-responsive dimming and blind control system. Prototypes of such systems have been tested (Lee & al., 1998) and are currently coming to the market.
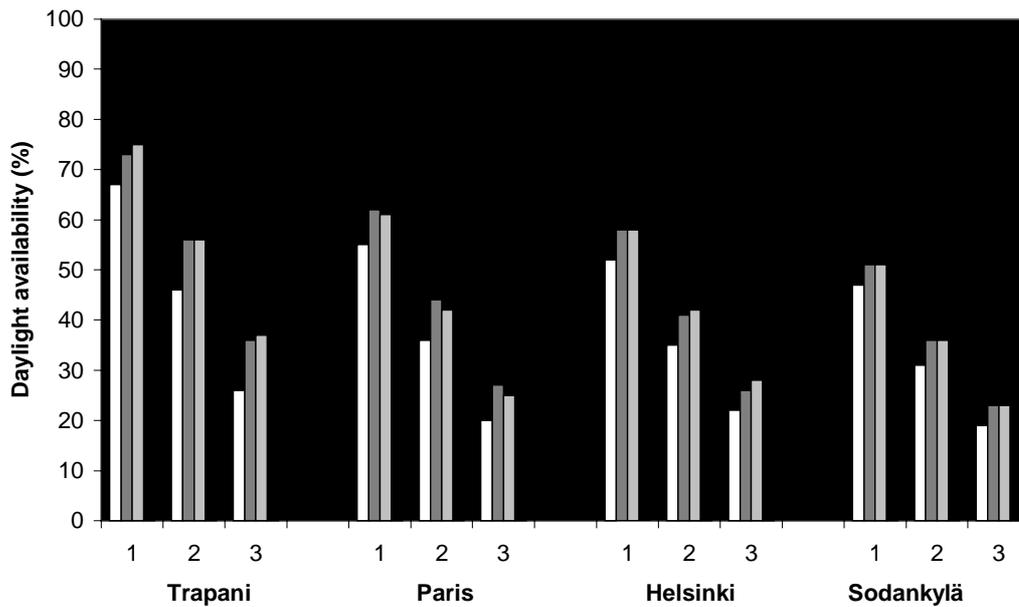
Fig. 13. The yearly average daylight availability *DA* (in % of the lighting requirement during the office hours) for different electric light control strategies: 1) continuous dimming; 2) on/half/off switching; 3) on/off switching at four locations and for different facade orientations: white = south, dark grey = west, light grey = east, black = north.

4.8 Utilizing the beam sunlight: diffusive glazing elements

From Figs 7 and 13 it is clear that the behaviour of the occupants controlling the blinds and electric light switches is a key variable affecting the interior daylight availability. An automated, continuous daylight-responsive control system is an obvious way of increasing the daylight utilization. However, it would be simpler and easier for the occupants if a passive beam sunlight control system not requiring intervention by the occupants could be used. One way of achieving this would be to use diffusive glazing elements. Diffusive elements will diffuse all incoming beam, diffuse, and ground-reflected daylight. However, it is not possible to have a clear outside view through the diffusing elements: therefore, they should be positioned above the clear glazing window in the facade. Fig. 14 shows one possible layout of a solar facade with diffusive glazing elements. The window at the centre has an area of 14% of the total facade area which can be regarded as a minimum window area offering an adequate outside view. The diffusing element directly above the window has an area of 10% of the total facade area. The window at the centre together with the top centre diffusive element have an overall area equivalent to the base case window in the previous calculations (24%). In addition to the top centre diffusive element, it is possible to place diffusive elements at the top corners of the facade, giving an overall glazing area of 40% of the total facade area.
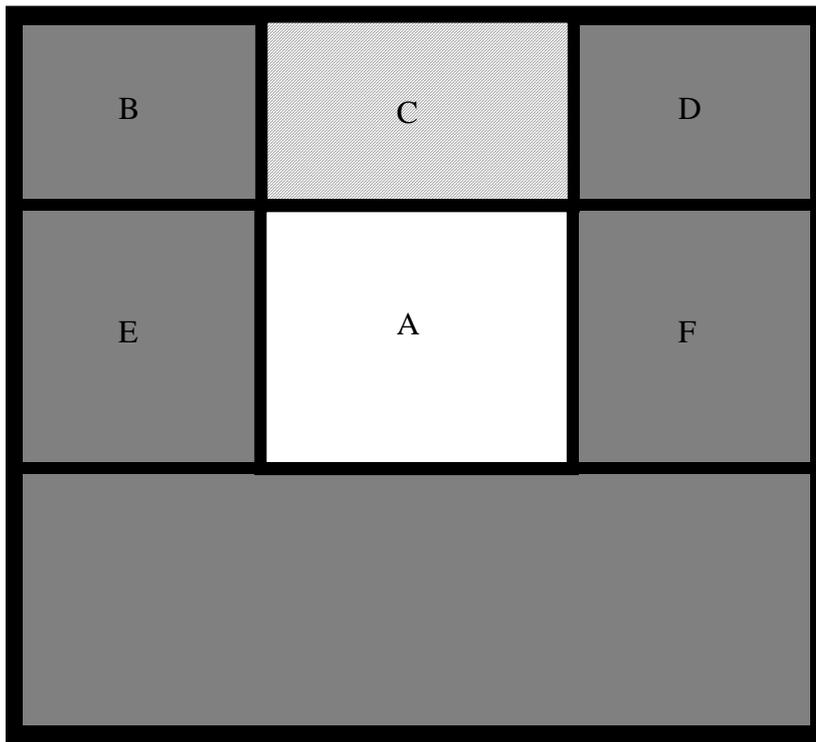
Fig. 14. Layout of a facade with diffusive glazing above the window. The symbols of the various parts of the facade (letters A-F) correspond to the results of Table 12.

The daylight availability of the diffusing elements with and without the centre window is presented in Table 12 (publication **I**). The calculations are based on the assumption that the diffusive glazing is ideally diffusing with a transmittance equal to that of the window. Blinds are applied only to the central clear glazing window and continuous dimming of electric light is used. The *DA*s without the window are shown just to indicate how much daylight they can provide; it is not suggested that a facade without a clear glazing window should be applied.

From Table 12 it can be seen that the top centre diffusive glazing (C) alone will produce more daylight than the clear glazing window (A) for south-, west-, and east-facing rooms in Trapani; the diffusive glazing does not require the blinds used with the clear glazing window, making available much unexploited beam and diffuse daylight. For the other locations, the diffusive glazing C is also better than the window for south-oriented facades, but for east- and west-oriented facades there is not much difference since they receive less beam sunlight. For north-facing facades, the window is always better than the diffusive glazing C because it is bigger and the north-facing facade receives no beam sunlight during the office hours.

Table 12. The yearly average daylight availability *DA* (in % of the lighting requirement during the office hours) for different diffusive glazing facade layouts at four locations and for different facade orientations, S = south, W = west, E = east, N = north

Facade layout	Trapani (38°)				Paris (49°)				Helsinki (60°)				Sodankylä (67°)			
	S	W	E	N	S	W	E	N	S	W	E	N	S	W	E	N
Window (A)	47	54	54	73	39	45	44	59	37	42	43	54	34	37	37	47
Base case	67	73	75	91	55	62	61	76	52	58	58	69	47	51	51	60
Centre diff.(C)	86	66	63	45	67	46	50	32	57	42	43	32	49	37	37	27
A+C	94	90	88	91	78	72	75	76	69	66	66	69	62	58	58	60
All diff.(BCD)	96	93	90	86	84	74	78	68	71	66	66	63	63	58	58	54
A+BCD	97	97	95	95	88	84	86	84	77	75	75	75	69	67	66	66
A+BCD+EF	98	98	97	97	94	90	92	89	82	81	80	81	73	72	72	72

Combining the window and the diffusive glazing (A+C) almost doubles the daylight availability for south-oriented facades, compared with the window alone. For east- and west-oriented facades, layout A+C increases the *DA* 21-36% points, and for north-oriented facades, 13-17%. Compared with a clear glazing window of equal area (24% of the total facade area), the layout A+C gives 15-27% points higher *DA* for south-oriented facades and 7-17% points higher *DA* for east- and west-oriented facades. For north-oriented facades, there is no difference since there is no beam sunlight available.

If diffusive glazing were also added to the top corners of the facade, the glazing area increases to 40% of the total facade area. This facade layout (A+BCD) would further increase the *DA* 3-7% points for Trapani and 6-12% points for the other locations. Increasing the glazing area further to 60%, by adding diffusive glazing to both sides of the window (layout A+BCD+EF), would increase the *DA* only a further 1-6% points. However, the layout A+BCD+EF is not realistic without blinds on diffusive glazing E and F. The luminance of the diffusive glazing could be as high as 10000 cd/m^2 in direct sunlight which could cause glare for the occupants. Therefore, clear glazing with blinds should always be used in the sections E and F beside the central window A (publication **VI**). The luminance of the diffuse sky alone is not likely to exceed 1000 cd/m^2 in most cases.

4.9 Summary of the parameters

The following conclusions can be made from the preceding analysis:

- Continuous dimming system is essential for full daylight utilization. With on/off control strategy, 20-60% of the useful daylight replacing the electric lighting is lost. With on/half/off control strategy, the *DA* is 65-90% of the *DA* of continuous dimming. The more frequently the electric lights are adjusted, the more daylight can be utilized.

- Shading system for the beam sunlight is necessary during the office hours for other than northern facade orientations because beam sunlight can cause glare for the occupants. However, valuable diffuse daylight is also lost with the shading system. If the blinds are totally closed when the sun shines in, 60-90% of the useful daylight will be lost in south-facing rooms. In east- and west-facing rooms, the *DA* could be increased by 30-60% with automated daylight-responsive blind control system.

- The *DA* is 10-20% points higher for north-facing than south-facing rooms because no blinds are needed on the north-facing windows during the office hours. This makes northern facades ideal for daylighting with clear glazing windows. For other orientations, diffusive glazing could be used at the top section of the facade. However, it is important to also have a clear glazing window to provide an outside view for the occupants.

- Diffusive glazing without blinds should not be used in the lower facade sections because the high luminance of the glazing could cause glare in direct sunlight. Diffusive glazing at the top section of the facade is not likely to cause glare for the occupants.

- The window sill should be positioned above the interior desk level. The higher the window is placed, the more uniform interior daylight distribution is achieved. A high and narrow window will bring more daylight to the back part of the room than a low and wide window.

- Daylighting is better suited for office buildings than domestic houses because the daylight availability coincides better with the office hours. The *DA* for the office hours (9-17) is 20-50% points more than for a typical domestic occupancy schedule.

- Increasing the window area increases the *DA* but it also increases the heating and cooling load. Moreover, a larger window leaves less room for other solar components, e.g. photovoltaic panels. The optimal window area with maximum energy benefits is analysed in section 5.

5 OPTIMIZATION OF SOLAR PV FACADES

It is clear from the previous section that by increasing the window area, it is possible to increase the interior daylight availability (*DA*), and simultaneously, to decrease the need for artificial lighting. However, beyond a certain point, enlarging the window increases the *DA* only marginally. On the other hand, enlarging the window reduces the facade area available for other solar components, e.g., photovoltaic (PV) panels which are used to produce electricity for the appliances in the building. Moreover, enlarging the window increases the heat losses during the winter and cooling load during the summer. Therefore, optimizing the window area becomes a question of minimizing the auxiliary energy requirement, or, maximizing the energy benefit of the facade. The electricity benefits of daylight and PV are assessed in section 5.1, the total auxiliary energy requirement, including heating and cooling energy, in section 5.2, and a sensitivity analysis of the modelling approach is presented in section 5.3.

5.1 Electricity benefits of daylight and PV

To illustrate the optimization problem, a multifunctional PV facade is depicted in Fig. 15. The multifunctional facade is similar to the facade of Fig. 14 except that PV panels (light grey) are added to the facade section below the window (white). As was explained in the previous section, a small clear glazing window (14% of the total facade area) at the centre of the facade is necessary for an outside view. The rest of the facade area (dark grey) above and beside the window can be either PV or windows. The facade frames are depicted in black. In this section, the optimal facade layout giving the maximum electricity benefit of daylight and PV for four different locations is determined. Both the electric lighting energy savings by daylight and the electricity produced by the PV panels is considered in finding the optimal window and PV area.

One possibility would be to cover all the facade area above and beside the window by PV panels (Fig. 16a). That would give a maximum PV area but a minimum window area. A facade with a maximum window and minimum PV area is depicted in Fig. 16b where the facade area beside the central window is covered with clear glazing and the facade area above the window with diffusive glazing elements. Diffusive glazing is used in the top section instead of clear glazing because diffusive glazing gives much higher *DA* since no blinds are needed. In the middle section, clear glazing with blinds is used because the high luminance of the diffusive glazing without blinds could cause glare to the occupants (publication **VI**). Obviously, the optimal facade giving the maximum electricity benefit is somewhere between 16a and 16b (publications **VI** and **IX**).
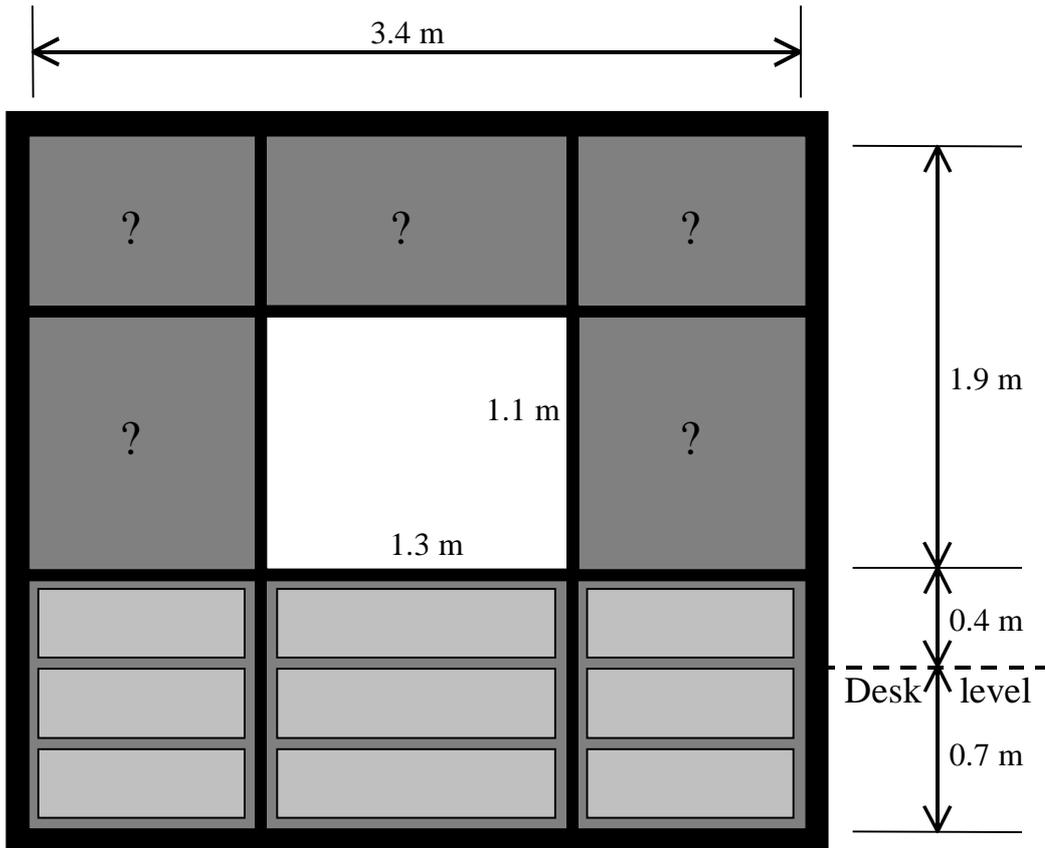
Fig. 15. A front view of a solar facade with a minimum window (white) and PV (light grey) area. The dark grey sections with question marks can be either PV or windows.

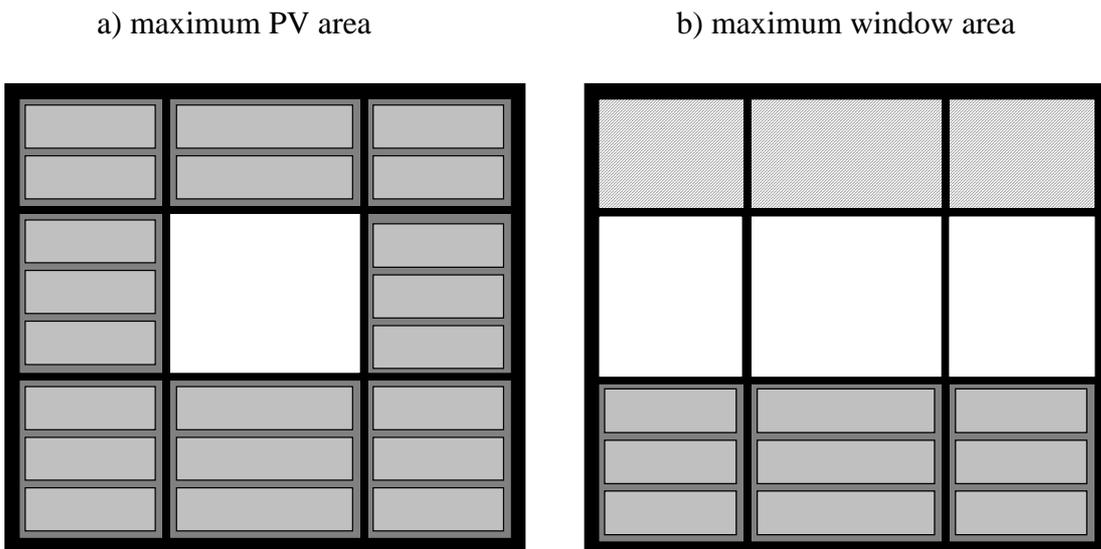a) maximum PV area   b) maximum window area

Fig. 16. A front view of a solar facade with a) a maximum PV and minimum window area, b) a maximum window and minimum PV area.

To determine the optimal window area, the yearly electricity benefit of daylight and PV is calculated for a south-facing facade at different locations and with different window areas. All the electricity produced by the PV panels of the facade during the office hours and the lighting electricity requirement replaced by daylight during the office hours is counted as beneficial. A luminous efficacy of 80 lm/W with a coefficient of utilization (CU) of 0.50 and a light loss factor (LLF) of 0.90 is assumed for the two electric luminaires. Continuous blind system control and continuous electric light dimming for both luminaires is assumed. The electric ballast of the dimming system is assumed to consume 10% of the full power when the electric light is dimmed totally off (publication **I**). The lighting requirement is 500 lx for the front and 300 lx for the back half of the room. Other input parameters were presented in Table 10.

The yearly electricity benefits for different window areas for a south-oriented facade in Trapani (a), Paris (b), Helsinki (c), and Sodankylä (d) are presented in Fig. 17. The window area is in % of the total facade area with the clear and diffusive glazing areas summed. The window area is first increased by putting diffusive glazing above the window and, beyond 40%, by putting clear glazing beside the window. The yearly electricity benefit is expressed in kWh per facade area. The white, bottom area represents the lighting electricity replaced by daylight. The dark grey area, second from bottom, represents the electricity produced by the PV panels if the system efficiency is 4%. The light grey area, third from bottom, and the medium grey, top area represent the additional PV electricity with system efficiencies of 8% and 12%, respectively.

As can be seen from the figures, the optimal window size is between 20% and 24% for all locations if PV with 12% system efficiency is used. A PV system efficiency of 12% corresponds to typical commercially available crystalline silicon (c-Si) PV modules. With 8% PV system efficiency, corresponding to triple-junction amorphous silicon (a-Si) PV, the optimal window area is slightly higher but the curve is flatter. With 4% PV system efficiency, corresponding to single-junction a-Si PV, the optimal window area is 26% for Trapani and around 32% for the other locations. However, the curve is very flat with window areas beyond 30% of the total facade area; the electricity benefit is not very sensitive to the window area with large windows and low PV efficiency.

It can be concluded that the optimal window area with high PV efficiency is very close to the layout of Fig. 14 where there is diffusive glazing above the central window, giving an overall glazing area of 24% of the total facade area. With low PV efficiency, the maximum electricity benefit would be achieved with most of the top modules replaced by diffusive glazing.
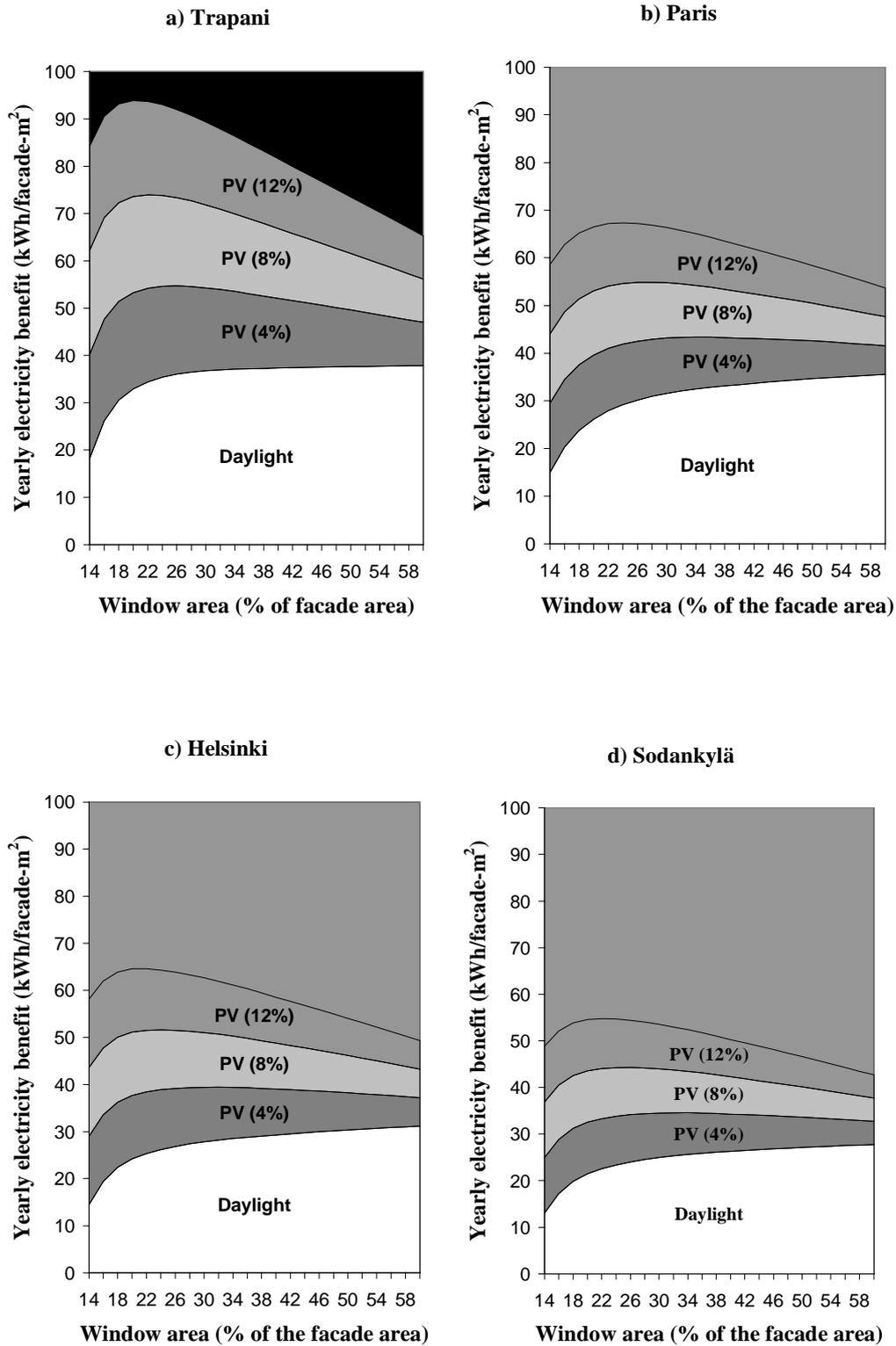
Fig. 17. Yearly electricity benefit of PV and daylight for a south-oriented facade in a) Trapani, b) Paris, c) Helsinki, and d) Sodankylä. The areas represent the electricity benefit of (from bottom to top): white - daylight; dark grey - PV if the system efficiency (η_{PV}) is 4%, light grey - if $\eta_{PV} = 8\%$, and medium grey - if $\eta_{PV} = 12\%$.

In the preceding optimization calculations, it has been assumed that PV modules will be installed only to the southern facade and all electricity produced by the PV panels can be consumed instantaneously inside the building so that no storage is needed. With the maximum PV area (60% of the total facade area), the maximum nominal PV power of the facade with 4% PV efficiency would be about 250 W or 15 W/m^2 of the southern floor area, which can easily be consumed in one room by, e.g., powering the office computer equipment. However, it would be interesting to know the optimal window area for facade orientations other than due south. The yearly electricity benefit as a function of the window area for south-, west-, east-, and north-oriented facades in Trapani is presented in Fig. 18.

It can be seen that the optimum window area for western, eastern, and northern facades in Trapani is between 24% and 34% of the total facade area, depending on the PV efficiency. Note that only the PV production during the office hours was included in the calculations. The inclusion of the PV production outside the office hours (mornings, evenings, and weekends) would slightly decrease the optimum facade area. The yearly PV production in four locations for west-, east-, and north-oriented facades as a percentage of the PV production for a south-oriented facade is presented in Table 13 for the office hours, other than office hours, and all hours.

Table 13. The yearly PV production in four locations for west-, east-, and north-oriented facades as a percentage of the PV production for a south-oriented facade (= 100%) for the office hours (Mon-Fri, 9-17), other than office hours (Mon-Fri, 0-9 & 17-24, and Sat & Sun, 0-24), and all hours (Mon-Sun, 0-24), W = west, E = east, N = north

Hours of PV production	Trapani (38°)			Paris (49°)			Helsinki (60°)			Sodankylä (67°)		
	W	E	N	W	E	N	W	E	N	W	E	N
Office hours	62	60	25	58	56	25	53	56	28	54	56	32
Other hours	106	114	47	169	60	57	113	89	51	115	107	70
All hours	78	79	33	102	58	40	77	69	38	79	77	48

It can be seen that the southern and northern facade together produce about the same amount of electricity as the eastern and western facade together in Trapani during the office hours, but the southern + northern facades produce about 10% more in Paris and about 20% more in Helsinki and Sodankylä than the eastern + western facade. However, if the PV production during all hours is included, the eastern + western facades produce 5-18% more than southern + northern facades, depending on the location.
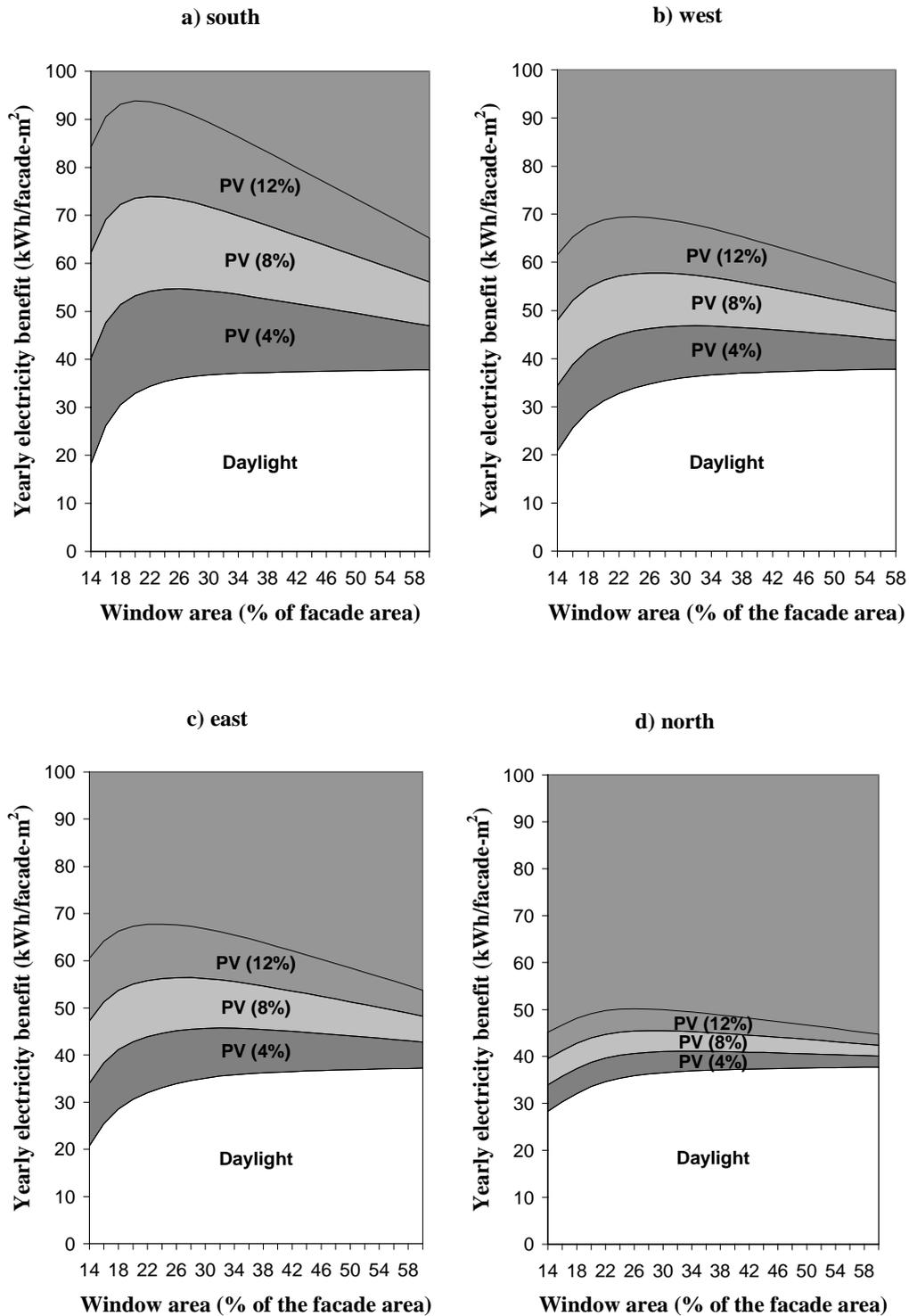
Fig. 18. Yearly electricity benefit of PV and daylight in Trapani for a) south-, b) west-, c) east-, and d) north-oriented facade. The areas represent the electricity benefit of (from bottom to top): white - daylight; dark grey - PV if the system efficiency (η_{PV}) is 4%, light grey - if $\eta_{PV} = 8\%$, and medium grey - if $\eta_{PV} = 12\%$.

In Paris where the afternoons are much less cloudy than the mornings, the western facade produces about the same amount of electricity as the southern facade during all hours. For the other locations, the southern facade orientation is clearly the best for the office hours and also for all hours. Therefore, if PV modules are installed only at one facade of the building, they should be installed at the southern facade.

The northern facade is optimal for clear glazing windows because it receives no beam sunlight during the office hours, and no blinds are needed. A possible optimal solution for an oblong building maximizing the daylight availability would be to have the long facades to south and north, with PV only on the southern facade. In this way, most of the building would receive daylight. An example of such building is presented in Fig. 19 where only the corridor does not receive daylight. The corridor C has only a small effect on the average daylight availability of the building because it is narrower than the rooms and the lighting requirement in the corridor is relatively small (publication **VI**). The dotted lines in Fig. 19 divide the rooms into two daylighting zones. The front halves A and E, which are closest to the windows have a higher lighting requirement than the back halves B and D.
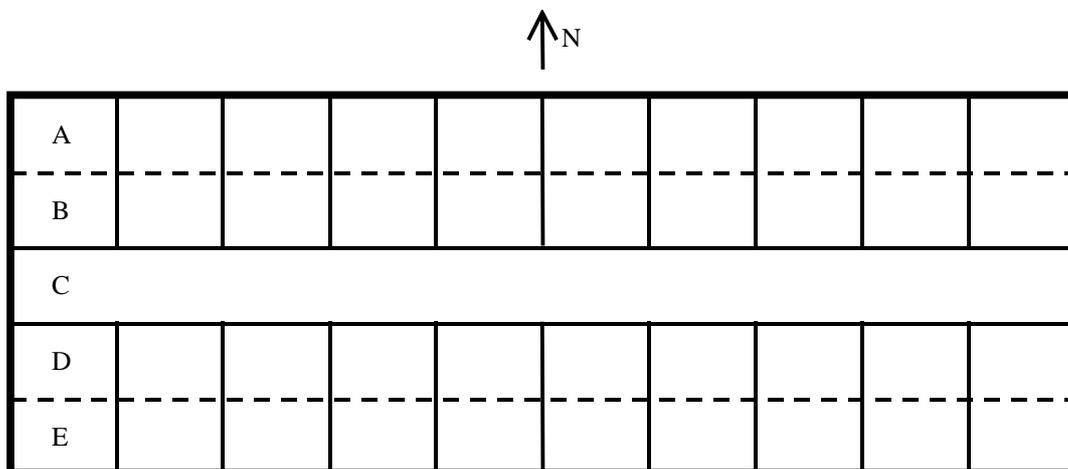

Fig. 19. An example layout of an oblong building maximizing the daylight availability. The front room halves A and E which are closest to the window have a higher lighting requirement (500 lx) than the back halves B and D (300 lx). The corridor C has an even lower lighting requirement (100 lx). PV panels are installed only at the southern facade of the building. (publication **VI**)

Because there is no PV on the northern facade, the PV electricity produced at the southern facade can be also used on the north-facing rooms. Therefore, all the electricity produced by PV modules with 8% system efficiency is likely to be consumed instantaneously inside the building during the office hours. With 12% PV efficiency, it is possible that all the produced electricity can not be utilized within the building and a storage or possibility to sell the electricity to the grid would be required. Same applies also if the PV production outside the office hours is counted as electricity benefit.

5.2 Discussion on heating and cooling energy

In the previous analysis, only electricity benefits of daylight and photovoltaics were included in the optimization of the facade window area. However, the effect of heating and cooling energy should also be considered. In this section, an indicative study with a very simple heating and cooling model is discussed, and in section 5.3, a sensitivity analysis of the simplified modelling approach is presented.

Increasing the facade window area will also increase the heat losses through the facade because the window has a larger heat transfer coefficient than the opaque wall. Moreover, the increased window area will increase the solar flux through the window, and therefore, increase the cooling load of the building, especially during the office hours. In the previous calculations, it was assumed that all beam radiation on the clear glazing window is reflected back by, e.g., Venetian blinds, resulting in only a part of the diffuse radiation entering the room. However, with diffusive glazing without the blinds, there is a significant solar heat flux into the building when the sun is shining, and the effect of cooling energy has to be considered.

It can be argued that a significant part of the solar radiation coming through the facade during the office hours, especially during the summer, is excess heat because the internal gains from the occupants, lighting, and other office appliances will more than offset the possible heat losses through the facade. However, outside the office hours there are no significant internal heat gains, and therefore, the effect of heating energy has to be included in the comparison between different window areas. Ventilation and infiltration will also affect the heating and cooling load of the building, but it is not easy to incorporate them in a simple model. For example, omission of the heat recovery effect of infiltrating/exfiltrating air and using a constant exfiltration rate tend to overestimate the calculated heating load (Virtanen, 1993). Therefore, in this simple model, it is assumed that ventilation and infiltration do not depend on the window area and the calculated heating and cooling energy for the different window areas is only an order-of-magnitude relative value. It is assumed that the same mechanical ventilation system is used for all window areas. A heat transfer coefficient of 1.5 W/m^{2}K for the

windows and 0.2 W/m^{2}K for the rest of the constructions is assumed for the calculations.

It is assumed that the office room temperature is kept between 18°C and 26°C. With lower temperatures than 18°C, auxiliary heating is needed, and with higher temperatures than 26°C, auxiliary cooling must be used. For the cooling electricity calculations, it is assumed that with an outdoor temperature below 17.5°C, the building can be cooled down with the outdoor air, but with higher outdoor temperatures, the indoor air must be refrigerated. With a temperature of 17.5°C, cold fresh air has a small allowance to heat up before reaching the ventilated space at the minimum room temperature. It is assumed that exhaust air can be used to heat the cold fresh air if necessary (Peippo & al., 1999). A constant coefficient of performance (COP, the ratio of the cooling load to the auxiliary cooling electricity) of 3 is assumed for the cooling load (Arkin & Navon, 1993), corresponding to a typical mechanical compression cooling system. In reality, the COP is not a constant but a function of the outdoor temperature, but a constant COP has been used in this simplified study. The equations for the hourly heating and cooling energy calculations can be found in publication **I**. It can be noted that a similar simplified method for the cooling calculations was presented by Santamouris and Asimakopoulos (1996) and the method was compared with the results of a more detailed TRNSYS simulation model. The annual cooling load for the simplified method agreed within 15% of the cooling load of the TRNSYS model. Moreover, the annual heating load of the simplified heating model agreed within 15% of the predicted heating load of a more detailed building energy simulation code FHOUSE (Aro-Heinilä and Suvanen, 1980) for a building of a low thermal mass (Peippo & al, 1999).

The yearly total relative auxiliary energy requirement for a south-oriented facade in Trapani, Paris, Helsinki, and Sodankylä is presented in Fig. 20. The cooling energy is in white, the heating energy in black, lighting electricity in white, and the auxiliary electricity required for the appliances (other than lighting) if the PV system efficiency (η_{PV}) is 12% is in medium grey. The additional auxiliary electricity for the appliances if η_{PV} = 8% is in light grey, and if η_{PV} = 4% in dark grey. It is assumed that all the PV electricity produced by the PV panels (both during and outside the office hours) can be used within the building or sold to the grid. The building is a multi-story office building with a similar layout as in Fig. 19. As there are no PV panels on the northern facade of the building, the PV electricity produced at the southern facade can be used also on the north-facing rooms. Therefore, the electricity required by the appliances is 30 W/m^2 (of the south-facing room area) which is double of the requirement for one room. Two computers in both south- and north-facing rooms are assumed to be switched on during the office hours, each computer having a power consumption of 125 W (Metsi & al., 1993).
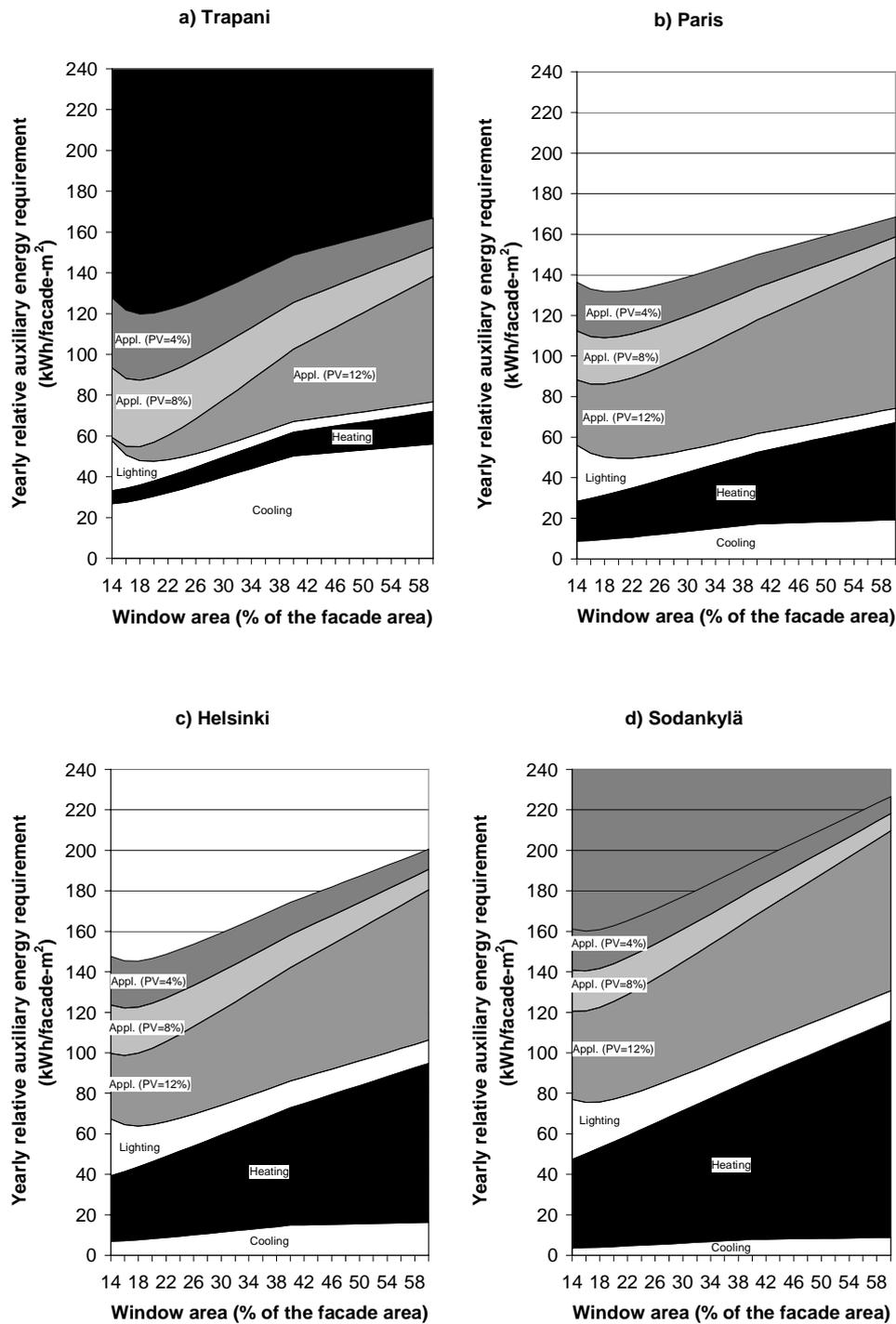
Fig. 20. Yearly relative auxiliary energy requirement for a south-oriented facade in a) Trapani, b) Paris, c) Helsinki, and d) Sodankylä. The areas represent the energy for (from bottom to top): white - cooling; black - heating; white - electric lighting; medium grey - appliances if the PV system efficiency (η_{PV}) is 12%, light grey - if $\eta_{PV} = 8\%$, and dark grey - if $\eta_{PV} = 4\%$. Diffusive glazing without blinds is added up to 40% of the facade area, and beyond 40%, clear glazing without blinds.

It can be seen that the optimal window area is between 14% and 20% of the total facade area for all PV efficiencies and locations, i.e., very close to the minimum window size. This is explained mainly by the increasing cooling load in the southern locations and heat losses in the northern locations with larger windows. While the heating and cooling energy increase fairly linearly with the window area, the required auxiliary lighting electricity decreases less with greater windows because most of the additional daylight is in excess of the requirement. Moreover, the cooling energy increases less with smaller windows because of the greater reduction of the heating load of the electric light. With window areas greater than 40% of the total facade area, the cooling energy increases very little because clear glazing with blinds instead of diffusive glazing without blinds is used in increasing the window area beyond 40%.

It is interesting to note from Fig. 20 that there is an optimal window area even for a facade without PV. The minimum auxiliary energy requirement for heating, cooling, and electric lighting is achieved with a window area of 16-20% of the total area of a south-oriented facade. For the other facade orientations, the PV electricity production is not as great as for the south, and PV is less cost-effective. For that reason, the relative auxiliary energy requirement for only heating, cooling, and electric lighting is presented in Fig. 21 for a north-oriented facade in Trapani (a) and Sodankylä (b).
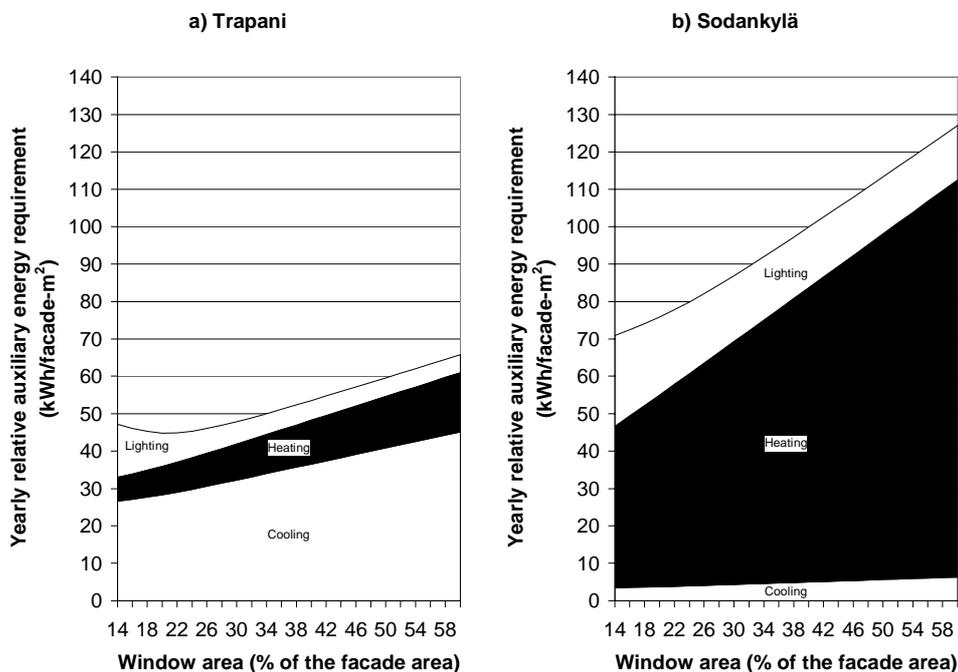

Fig. 21. Yearly relative auxiliary energy requirement for a north-oriented facade in a) Trapani and b) Sodankylä. The areas represent the energy for (from bottom to top): white - cooling; black - heating; white - electric lighting.

The auxiliary cooling energy is in white (bottom), heating energy in black, and the electricity for lighting in white (top) in Fig. 21. It can be seen that the optimum facade area for Trapani is 20%, but for Sodankylä, it is less than 14%. The increased heating requirement more than offsets the decreased auxiliary lighting requirement when the window area is increased in Sodankylä. The difference to the southern facade is that the daylight availability already is relatively high with a 14% north-oriented window because no blinds are necessary there, whereas with the south-oriented window, the *DA* can increase much more when diffusive glazing is added to the 14% clear glazing window with the blinds. In any case, the optimal window area seems to be rather close to the minimum (14% of the total facade area) for all facade orientations and locations.

5.3 Sensitivity analysis of the modelling approaches

It must be emphasized that in this study, a very simple model for the heating and cooling calculations has been used, compared with the detailed daylight modelling which has been the main subject of the thesis. Therefore, the presented optimal window areas must be seen as indicative rather than definite results. In addition to the accuracy of the model, the choice of the modelling approach could affect the results. For example, in this study, it has been assumed that electricity and heating energy are equal, i.e., the electricity has been generated with a conversion factor of 1. However, it can be argued that electricity is more valuable if it is generated with a lower conversion factor. For example, a typical conversion factor for a condensing power plant is close to 0.35 (Peippo & al., 1999). That would make electricity almost three times as valuable as heat in terms of primary energy consumption. For this reason, the yearly relative auxiliary energy in Helsinki (Fig. 20c) and Sodankylä (Fig. 20d) is presented in Fig. 22 in terms of electricity consumption where a conversion factor of 0.35 from heat to electricity is used.

It can be seen that the optimum window area is now 1-2% points greater than in Fig. 20 where a conversion factor of 1 was used. The effect of the conversion factor for Trapani and Paris would be even smaller because they have much smaller heating loads than the Finnish locations. In addition to the conversion factor from heat to electricity, the COP of the cooling system could affect the optimal window area. A COP of 3 was used in the previous calculations (Fig. 20). To analyse the effect of the COP, the yearly relative auxiliary energy requirement in Trapani for COPs of 2 and 4 is presented in Fig. 23. It can be seen that the optimal window area is about 2% points greater for the cooling system with a COP of 4 than a system with a COP with 2. The effect of the COP is smaller for the other locations since they have much smaller cooling loads than Trapani.
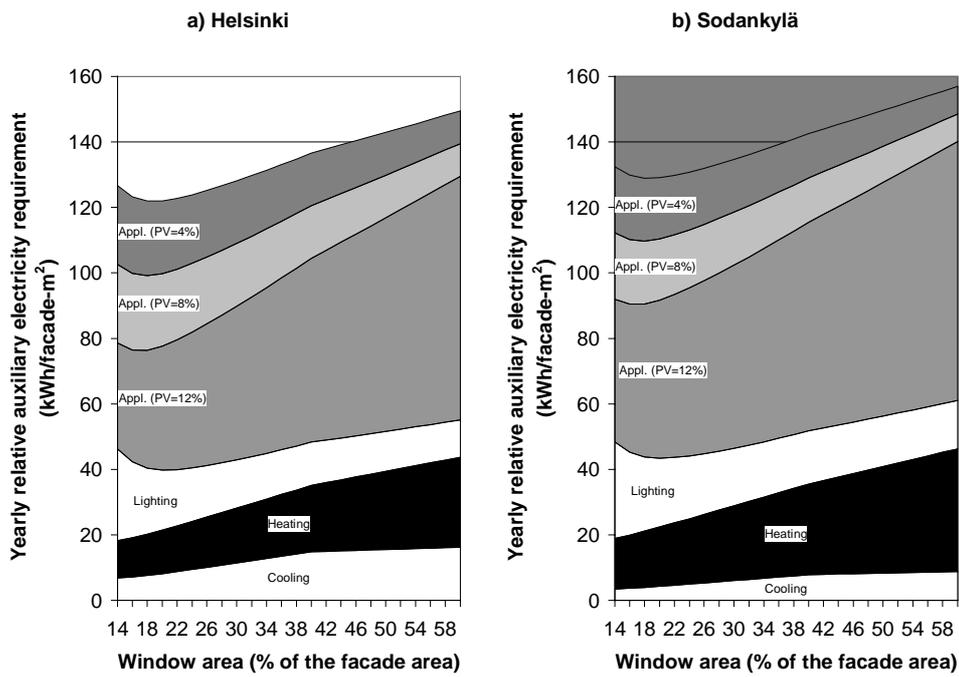
Fig. 22. Yearly auxiliary electricity requirement (with a conversion factor of 0.35 from heat to electricity) for a south-oriented facade in a) Helsinki and b) Sodankylä.
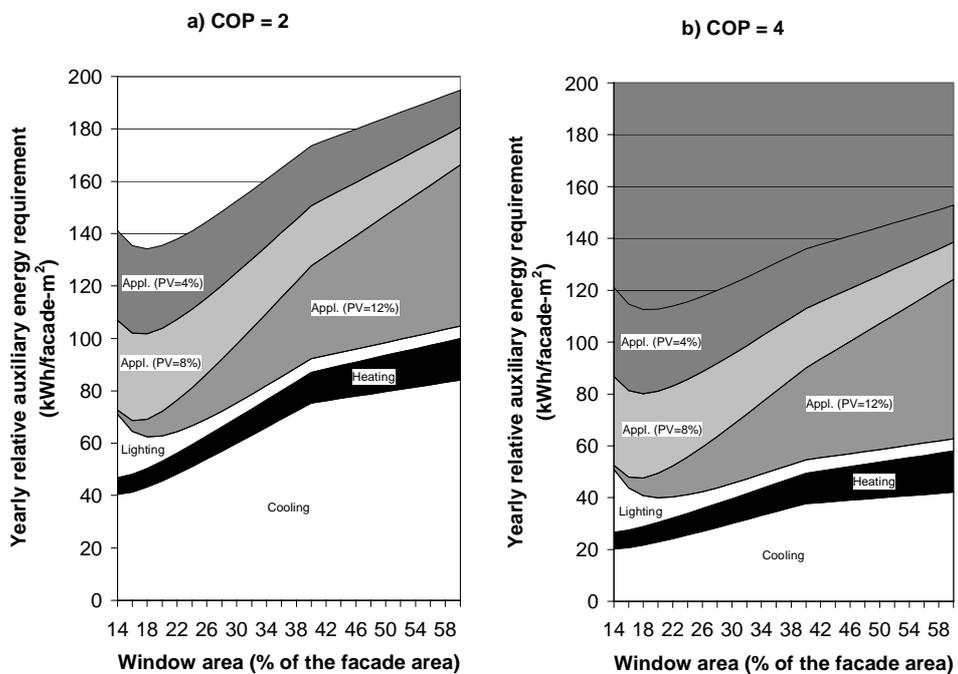

Fig. 23. Yearly auxiliary energy requirement for a south-oriented facade in Trapani with different cooling systems: a) COP = 2, b) COP = 4.

Another factor that could effect the optimal window area is the PV electricity production outside the office hours. This amounts to 35-40% of the total PV electricity, depending on the location. If the electricity can not be stored or sold to the grid, then the PV electricity produced outside the office hours can not be counted as benefit. For this reason, the yearly relative auxiliary energy requirement in Trapani (Fig. 20a) and Helsinki (Fig. 20c) is presented in Fig. 24 with only the PV electricity production during the office hours counted as benefit. It can be seen that the effect of the PV electricity production outside the office hours on the optimal window area is 1-2% points of the total facade area. The effect for the other locations is about the same.
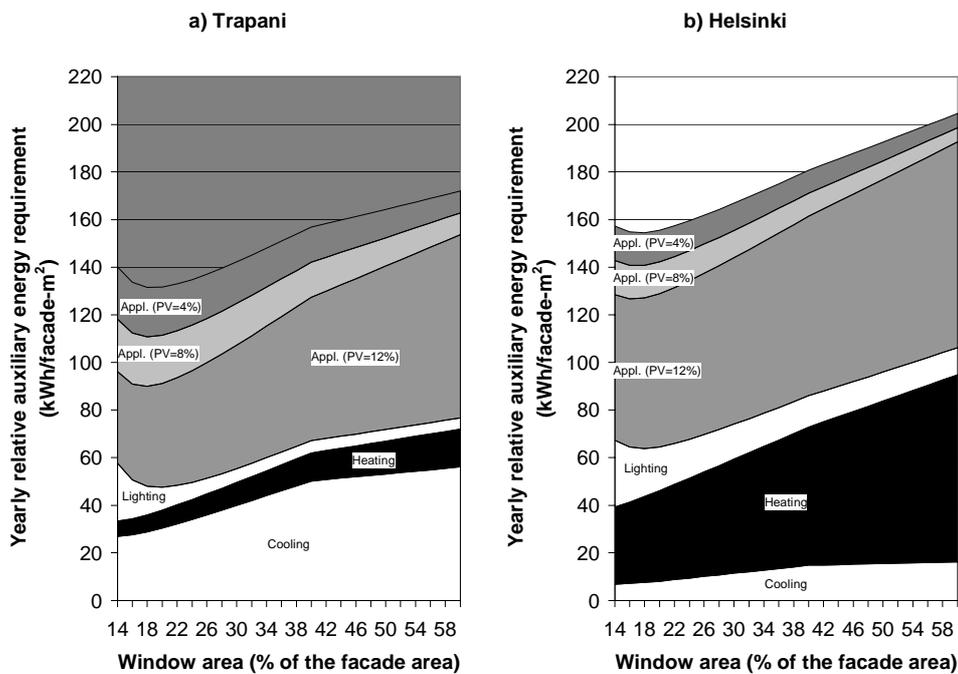

Fig. 24. Yearly auxiliary energy requirement for a south-oriented facade in a) Trapani, b) Helsinki with only the PV electricity produced during the office hours counted as benefit. The areas represent the electricity for (from bottom to top): white - cooling; black - heating; white - electric lighting; medium grey - appliances if the PV system efficiency (η_{PV}) is 12%, light grey - if $\eta_{PV} = 8\%$, and dark grey - if $\eta_{PV} = 4\%$.

It can be concluded that the optimal window area does not seem to be very sensitive to the variation in the heating, cooling, and PV electricity production modelling approach. In this indicative study, the optimal window area would appear to be 15-20% of the total facade area for most cases, corresponding to 7-10% of the total floor area of the building. This is fairly close to the optimal total window area (5-6% of the floor area) arrived at by Peippo & al. (1999) where a simple daylight factor model was used for the daylight calculations. For a more accurate window area optimization, also a more detailed heating and cooling model would be needed.

6 CONCLUSIONS

In this thesis, the daylight availability and energy benefits of daylighting in solar facades have been assessed. The various parameters affecting the yearly average daylight availability (*DA*), e.g. location, orientation, window area, window position, electric light control, and shading system, have been analysed. The following conclusions have been made:

- *Continuous dimming system* is essential for full daylight utilization. With on/off control strategy, 20-60% of the useful daylight replacing the electric lighting is lost. With on/half/off control strategy, the *DA* is 65-90% of the *DA* with continuous dimming. The more frequently the electric lights are adjusted, the more daylight can be utilized.

- *Blind system for the beam sunlight* is necessary during the office hours for other than northern facade orientations because beam sunlight can cause glare for the occupants. However, valuable diffuse daylight is also lost with the shading system. If the blinds are totally closed when the sun shines in, 60-90% of the useful daylight will be lost in south-facing rooms. In east- and west-facing rooms, the *DA* could be increased by 30-60% with automated daylight-responsive blind control system.

- The *DA* is 10-20% points higher for north-facing than south-facing rooms because no blinds are needed on the north-facing windows during the office hours. This makes northern facades ideal for daylighting with clear glazing windows. For other orientations, diffusive glazing could be used at the top section of the facade. However, it is important to also have a clear glazing window to provide an outside view for the occupants.

- Diffusive glazing without blinds should not be used in the lower facade sections because the high luminance of the glazing could cause glare in direct sunlight. Diffusive glazing at the top section of the facade is not likely to cause glare for the occupants.

- The window sill should be positioned above the interior desk level. The higher the window is placed, the more uniform interior daylight distribution is achieved. A high and narrow window will bring more daylight to the back part of the room than a low and wide window.

- Daylighting is better suited for office buildings than domestic houses because the daylight availability coincides better with the office hours. The *DA* for the office hours (9-17) is 20-50% points more than for a typical domestic occupancy schedule.

- Increasing the window area increases the *DA*, but it also increases the heating and cooling load. The optimal window size for a south-oriented multifunctional photovoltaic (PV) facade, giving the minimum auxiliary energy requirement for heating, cooling, and electricity for lighting and other appliances, was around 15-20% of the total facade area for most cases in an indicative study including four European locations. For other facade orientations, the PV electricity production is less than for the south and it might not be useful to put PV on them.

For the daylight availability calculations in this thesis, a new daylight simulation tool DeLight, developed at Helsinki University of Technology, was used. DeLight uses hourly horizontal diffuse and beam irradiance measurements as input data. The irradiance measurements are converted to illuminance values by a luminous efficacy model. The illuminance values are used to generate a sky luminance distribution by a sky luminance model. The interior daylight illuminance is calculated from the room geometry and the sky luminance distribution by an interior light transfer model.

In the process of developing the model, some important observations have been made:

- Neglecting the *shadow ring correction* of the input diffuse irradiance measurements can lead to an average underestimation of 20% of the diffuse irradiance component.

- Using a constant *luminous efficacy model* in converting the input irradiance data to illuminance values will underestimate the diffuse daylight illuminance by about 15%. The Perez luminous efficacy model was found to agree best with the measurements.

- The Perez all-weather *sky luminance model* was found to agree best with the measurements. Using an isotropic sky model would underestimate the diffuse component by an average of 25% on a south-oriented surface.

The simulation tool DeLight has been verified with year-round illuminance and irradiance measurements. The average error of simulated interior daylight illuminances is only 2-3% with typical lighting requirement levels (300-500 lx). The average simulation time of all hours of the year is only 1-2 minutes with DeLight. The relatively good accuracy and speed make it a useful tool for daylight modelling and optimization studies.

A possible object for future development of DeLight could be the inclusion of skylight windows. Another interesting topic would be detailed modelling of various shading systems and also more advanced daylighting techniques, such as light shelves. Finally, a more detailed heating and cooling energy model would be required for accurate multifunctional facade optimization studies.

REFERENCES

Arkin H. & Navon R., 1993. Evaluation of two unitary cooling systems for residences in Eilath (Israel). *Proceedings of the 6th International Conference on Indoor Air Quality and Climate, Helsinki, Finland, July 4-8*. Vol. **5**, p. 407-412.

Aro-Heinilä V. & Suvanen M., 1980. *Simulation program for energy analysis of multiroom houses for solar energy studies*. Report TKK-F-A436, Helsinki University of Technology, Espoo.

Arpiainen, Sanna, 1999. A comparison of daylight illuminance measurements with interior illuminance distributions calculated by Adeline and DeLight simulation programs (in Finnish: *'Päivänvalon valaistusvoimakkuuden mittausten vertailu Adeline-ja DeLight-simulointiohjelmien laskemiin jakaumiin huoneen sisällä'*). Special assignment, Helsinki University of Technology, Department of Engineering Physics and Mathematics, Otaniemi, Finland, 36p.

Brunger, Alfred P. & Hooper, Frank C., 1993. Anisotropic sky radiance model based on narrow field of view measurements of shortwave radiance. *Solar Energy*. Vol. **51**, nr 1, p. 53-64.

Bryan, Harvey J. & Clear, Robert D., 1981. Calculating interior daylight illumination with a programmable hand calculator. *Journal of the Illuminating Engineering Society*. Vol. **10**, nr 4, p. 219-227.

Bülow-Hübe, Helena, 2000. Office worker preferences of exterior shading devices: a pilot study. *Proceedings of the 3rd ISES-Europe Solar Congress, EuroSun 2000, Copenhagen, Denmark, June 19-22*.

CEC, 1993. *Daylighting in architecture - a European reference book*. Commission of the European Communities, Directorate-General XII for Science, Research and Development. London, UK: James & James.

Choi A. & Mistrick R.G., 1997. On the prediction of energy savings for a daylight dimming system. *Journal of the Illuminating Engineering Society*. Vol. **26**, nr 2, p. 77-90.

Chung T.M., 1992. A study of luminous efficacy of daylight in Hong Kong. *Energy and Buildings*. Vol. **19**, nr 1, p. 45-50.

CIBSE, 1984. *CIBSE code for interior lighting 1984*. The Chartered Institution of Building Services Engineers, London, UK.

IEA, 1994. *Passive solar commercial and institutional buildings - a sourcebook of examples and design insights*. International Energy Agency. John Wiley & Sons Ltd, Chichester, UK, 454 p.

IEA, 1999. *Daylighting simulation: methods, algorithms, and resources*. A report of IEA SHC Task 21 / ECBCS ANNEX 29. Lawrence Berkeley National Laboratory, Berkeley, CA, USA.

IESNA, 1993. *Lighting handbook*. 8th edition, Illuminating Engineering Society of North America, New York, NY, USA.

Gillette G.L. & Treado S.J., 1985. Correlations of solar irradiance and daylight illuminance for building energy analysis. *ASHRAE Transactions*. Vol. **91**, nr 1A, p. 180-192.

Kipp & Zonen. *Directions for use: Pyranometer with shadow ring CM 11/121*.

LeBaron B. A., Michalsky J. J. & Perez R., 1990. A simple procedure for correcting shadowband data for all sky conditions. *Solar Energy*. Vol. **44**, nr 4, p. 249-256.

Lee E.S., DiBartolomeo D.L., & Selkowitz S.E., 1998. Thermal and daylighting performance of an automated venetian blind and lighting system in a full-scale private office. *Energy and Buildings*. Vol. **29**, nr 1, p. 47-63.

Littlefair, Paul J., 1985. The luminous efficacy of daylight: a review. *Lighting Research & Technology*. Vol. **17**, nr 4, p. 162-182.

Littlefair, Paul J., 1988. Measurements of the luminous efficacy of daylight. *Lighting Research & Technology*. Vol. **20**, nr 4, p. 177-188.

Littlefair, Paul J., 1990. Innovative daylighting: review of systems and evaluation methods. *Lighting Research & Technology*. Vol. **22**, nr 1, p. 1-17.

Littlefair, Paul J., 1994. A comparison of sky luminance models with measured data from Garston, United Kingdom. *Solar Energy*. Vol. **53**, nr 4, p. 315-322.

Lynes, J.A., 1996. Daylight and photometric anomalies. *Lighting Research & Technology*. Vol. **28**, nr 2, p. 63-67.

Metsi P., Pihala H. & Wilkins K., 1993. Measurement of office buildings equipment loads. *Proceedings of the 6th International Conference on Indoor Air Quality and Climate, Helsinki, Finland, July 4-8*. Vol. **5**, p. 437-442.

Olseth J.A. & Skartveit A., 1989. Observed and modelled hourly luminous efficacies under arbitrary cloudiness. *Solar Energy*. Vol. **42**, nr 3, p. 221-233.

Muneer T. & Kinghorn D., 1998. Luminous efficacy models: evaluation against UK data. *Journal of the Illuminating Engineering Society*. Vol. **27**, nr 1, p. 163-170.

Peippo K., Lund P.D. & Vartiainen E., 1999. Multivariate optimization of design trade-offs for solar low energy buildings. *Energy and Buildings*. Vol. **29**, nr 2, p. 189-205.

Perez R., Ineichen P., Seals R., Michalsky J. & Stewart R., 1990. Modeling daylight availability and irradiance components from direct and global irradiance. *Solar Energy*. Vol. **44**, nr 5, p. 271-289.

Perez R., Seals R. & Michalsky J., 1993a. All-weather model for sky luminance distribution - preliminary configuration and validation. *Solar Energy*. Vol. **50**, nr 3, p. 235-245.

Perez R., Seals R. & Michalsky J., 1993b. Erratum to All-weather model for sky luminance distribution - preliminary configuration and validation. *Solar Energy*. Vol. **51**, nr 5, p. 423.

Pleijel, Gunnar, 1954. *The computation of natural radiation in architecture and town planning*. Statens nämd för byggnadsforskning. Meddelande 25, Stockholm, Sweden, p. 31, 82.

Rutten A.J.F., 1990. Sky luminance measurements for design and control of indoor daylight illumination. *Lighting Research & Technology*. Vol. **22**, nr 4, p. 189-192.

Santamouris M. & Asimakopoulos D., 1996. *Passive cooling of buildings.* James & James, London, UK, 472 p.

Saraiji R.M.N. & Mistrick R.G., 1993. The evaluation of determinant sky parameters for daylighting CUs. *Journal of the Illuminating Engineering Society*. Vol. **22**, nr 1, p. 131-138.

Secker, Sheila M. & Littlefair, Paul J., 1987. Daylight availability and lighting use: geographical variations. *Lighting Research & Technology*. Vol. **19**, nr 2, p. 25-34.

Suomen Standardisoimisliitto SFS, 1992. *Electrotechnical vocabulary. Lighting*. Standard SFS-IEC 50-845, Helsinki, Finland.

Suomen Sähkölaitosyhdistys, 1995. *Energiauutiset*. Nr 1, p. 26-29.

Suomen Valoteknillinen Seura, 1986. *Valaistussuositukset: sisävalaistus*. Suomen Valoteknillinen Seura r.y:n julkaisuja, nro 9-1986, Helsinki, Finland.

Tregenza P.R., 1980. The daylight factor and actual illuminance ratios. *Lighting Research & Technology*. Vol. **12**, nr 2, p. 64-68.

University of California, 1993. *Radiance user manual*. Lawrence Berkeley Laboratory, University of California, CA, USA.

Vartiainen, Eero, 1996. Utilization of daylight in interior lighting (in Finnish: '*Päivänvalon hyödyntäminen sisävalaistuksessa*'). Licentiate thesis, Helsinki University of Technology, Department of Engineering Physics and Mathematics, Otaniemi, Finland, 105p.

Vine E., Lee E., Clear R., DiBartolomeo D. & Selkowitz S., 1998. Office worker response to an automated venetian blind and electric lighting system: a pilot study. *Energy and Buildings*. Vol. **28**, nr 2, p. 205-218.

Virtanen, Markku, 1993. Thermal coupling of leakage air and heat flows in buildings and building components. Development and application of numerical models. *VTT Publications* 134, Espoo, Finland, 180 p.